BAMS Article

Differing Trends in United States and European Severe Thunderstorm Environments in a Warming Climate

Mateusz Taszarek, John T. Allen, Harold E. Brooks, Natalia Pilguj, and Bartosz Czernecki

ABSTRACT: Long-term trends in the historical frequency of environments supportive of atmospheric convection are unclear, and only partially follow the expectations of a warming climate. This uncertainty is driven by the lack of unequivocal changes in the ingredients for severe thunderstorms (i.e., conditional instability, sufficient low-level moisture, initiation mechanism, and vertical wind shear). ERA5 hybrid-sigma data allow for superior characterization of thermodynamic parameters including convective inhibition, which is very sensitive to the number of levels in the lower troposphere. Using hourly data we demonstrate that long-term decreases in instability and stronger convective inhibition cause a decline in the frequency of thunderstorm environments over the southern United States, particularly during summer. Conversely, increasingly favorable conditions for tornadoes are observed during winter across the Southeast. Over Europe, a pronounced multidecadal increase in low-level moisture has provided positive trends in thunderstorm environments over the south, central, and north, with decreases over the east due to strengthening convective inhibition. Modest increases in vertical wind shear and storm-relative helicity have been observed over northwestern Europe and the Great Plains. Both continents exhibit negative trends in the fraction of environments with likely convective initiation. This suggests that despite increasing instability, thunderstorms in a warming climate may be less likely to develop due to stronger convective inhibition and lower relative humidity. Decreases in convective initiation and resulting precipitation may have long-term implications for agriculture, water availability, and the frequency of severe weather such as large hail and tornadoes. Our results also indicate that trends observed over the United States cannot be assumed to be representative of other continents.

KEYWORDS: Lightning; Thunderstorms; Tornadoes; Climate change; Reanalysis data; Trends

https://doi.org/10.1175/BAMS-D-20-0004.1
Corresponding author: Mateusz Taszarek, mateusz.taszarek@amu.edu.pl
Supplemental material: https://doi.org/10.1175/BAMS-D-20-0004.2

In final form 3 August 2020

AFFILIATIONS: Taszarek—Department of Meteorology and Climatology, Adam Mickiewicz University, Poznan, Poland, National Severe Storms Laboratory, Norman, Oklahoma, and Cooperative Institute for Mesoscale Meteorological Studies, University of Oklahoma, Norman, Oklahoma; **Allen**—Central Michigan University, Mount Pleasant, Michigan; **Brooks**—National Severe Storms Laboratory, and School of Meteorology, University of Oklahoma, Norman, Oklahoma; **Pilguj**—Department of Climatology and Atmosphere Protection, University of Wrocław, Wrocław, Poland; **Czernecki**—Department of Meteorology and Climatology, Adam Mickiewicz University, Poznan, Poland

Increases to the frequency and intensity of severe thunderstorms are an expected outcome of anthropogenic warming over North America and Europe by 2100 (Diffenbaugh et al. 2013; Hoogewind et al. 2017; Allen 2018; Rädler et al. 2019; Trapp et al. 2019). However, detecting historical changes to the frequency of convective events has proven challenging, as direct observations are incomplete (Allen and Tippett 2015; Groenemeijer et al. 2017; Edwards et al. 2018; Chernokulsky et al. 2019; Taszarek et al. 2019). In the United States, changes in how tornadoes are reported have made it difficult to detect credible trends despite increases in the variability of these events and the intensity of outbreaks since the 1970s (Brooks et al. 2014; Elsner et al. 2015; Tippett et al. 2016). Due to these limitations, a typical practice has been to consider trends over time in environments favorable to the development of severe storms (Mohr and Kunz 2013; Mohr et al. 2015; Pistotnik et al. 2016; Rädler et al. 2018; Taszarek et al. 2019, 2020). However, studies focusing predominantly on North America have failed to identify significant trends consistent with those expected by future climate projections (Gensini and Ashley 2011; Robinson et al. 2013; Allen et al. 2015; Gensini and Brooks 2018; Allen et al. 2020).

To provide the extended record for analysis of trends, reanalysis data have typically been used to characterize convective environment, as observed upper-air profiles are comparatively sparse (Brooks et al. 2003; Allen and Karoly 2014; Gensini et al. 2014; Taszarek et al. 2018; King and Kennedy 2019). These data are used to take an ingredient-based approach to identifying the bounding distribution of environments favorable to severe convection (Johns and Doswell 1992; Doswell et al. 1996). Four relevant factors are conditional instability, sufficient low-level moisture, an initiating mechanism, and vertical wind shear. Instability can be expressed by convective available potential energy (CAPE), which provides an estimate of vertically integrated buoyancy force acting on a rising air parcel. This parameter is typically used to approximate the potential strength of an updraft (w), via the relationship $w = \sqrt{2\text{CAPE}}$ (Emanuel 1994). The presence of CAPE is a necessary condition for thunderstorm development. However, no thunderstorm will form if convective initiation does not take place. Convective inhibition (CIN), quantifies the portion of the atmosphere where a rising air parcel experiences negative buoyancy before reaching an unstable layer, and thus requires external forcing to reach a level of free convection. An absolute CIN of around 75–100 J kg^{-1} can notably reduce chances for convective initiation despite ample CAPE (Bunkers et al. 2010; Gensini and Ashley 2011; Hoogewind et al. 2017; Taszarek et al. 2019). However, CIN alone should not be considered as a predictor of initiation, as other features such as dry-air entrainment or availability of sufficient synoptic-scale lift are also important factors (Trapp and Hoogewind 2016; Westermayer et al. 2017). A fourth ingredient, vertical wind shear, governs the organization of updrafts and enables formation of long-lived storm modes such as supercells or quasi-linear convective systems that are more capable of producing severe weather (Smith et al. 2012; Thompson et al. 2012; Guastini and Bosart 2016; Gatzen et al. 2020; Antonescu et al. 2020).

Our current expectations are that a wetter and more unstable troposphere in the future climate will lead to the environment being more conducive to deep moist

convection (Diffenbaugh et al. 2013; Agard and Emanuel 2017; Hoogewind et al. 2017; Allen 2018; Gensini and Mote 2015). However, whether convection initiates is a substantial limit on estimating thunderstorm occurrence from environments (Rasmussen et al. 2020). Since CIN depends on details in the thermodynamic structure, its accurate calculation requires high resolution in the lowest part of the atmosphere. Because of the limited boundary layer vertical resolution of current climate models and reanalyses, it is uncertain how well those models can assess changes in CIN. In this study, we consider long-term trends in parameters associated with severe thunderstorms over Europe and the United States, and investigate the role played by changes in CIN. Based on high-vertical-resolution reanalysis data (including 28 levels in the lowest 2 km of the atmosphere) we show that substantial increases in CIN may offset any gains in instability and even cause a net decrease in the number of thunderstorms. Knowledge of the historical changes in convective environments can help to better understand how CIN may potentially affect the frequency of severe thunderstorms in a warmer future climate. Positive trends in instability may not necessarily result in a higher number of storms, particularly when accompanied by a considerable increase in CIN.

Datasets and methodology

Reanalysis data. For the purposes of this study we used the fifth generation of the European Centre for Medium-Range Weather Forecasts (ECMWF) atmospheric reanalysis (ERA5; Hersbach et al. 2020) over a period of 41 years from 1979 to 2019. The dataset has a 0.25° horizontal grid spacing with 137 terrain-following hybrid-sigma model levels, which contrasts many earlier studies that have used fewer pressure levels for parcel computations. For both Europe and the United States the domain contains 149 meridional and 244 latitudinal grid points at 1-hourly temporal resolution. As a result, a total of 25.4 billion vertical profiles were postprocessed to derive descriptive convective parameters. All computations performed in this work are based on hourly resolution, which contrast prior studies that used daily or 6-hourly intervals. An aspect of diurnal cycle in convective variability (e.g., highest CAPE during the day) should be also considered when interpreting the results based on percentiles.

Lightning data. Cloud-to-ground (CG) lightning flash counts for the observational validation of trends were derived from the National Lightning Detection Network (NLDN; Cummins and Murphy 2009; Kingfield et al. 2017) for the years 1989–2018. Since detection efficiency of CG lightning has been more stable in NLDN over time compared to intracloud (IC) flashes (Koehler 2020), the latter was not taken into account. Flashes with a peak current lower than 15 kA were removed as many of them result from IC flashes (Wacker and Orville 1999; Kingfield et al. 2017; Medici et al. 2017; Koehler 2020). Detection efficiency of NLDN has improved from around 70% in 1989 (Orville 1991) to 95% since 2013 (Murphy and Nag 2015). In this study, lightning counts were summed on a 0.25° grid at the hourly step to match the ERA5 resolution.

Trend and parameter computations. The long-term climatology used herein is expressed by a fraction, frequency, or percentiles of a specific variable, which is then evaluated unconditionally or conditionally on covariate parameters. Trends at each grid point are then derived by obtaining values for each individual year and applying the nonparametric Sen's slope analysis (Wilcox 2010). We chose this metric due to its insensitivity to outliers and frequent application for evaluating robust trends in the atmospheric sciences. Significance of the trend is assessed using a two-tailed p value at the 0.05 threshold, and are denoted as "×" symbols in each figure. Slope units are normalized to correspond to changes over a period of 10 years. Following Rädler et al. (2019) we use the 50th percentile to investigate climatology and changes in a wind shear, and upper distributions (95th and 99.9th percentiles) for thermodynamic parameters.

For parcel parameter calculations, a surface to 500 m above ground level (AGL) mixed layer was used while also applying a virtual temperature correction (Doswell and Rasmussen 1994). CAPE is calculated using the vertical integral of positive parcel buoyancy (relative to the environment) from the lifted condensation level to equilibrium. CIN is calculated using the integral of negative parcel buoyancy between the mixed layer and the level of free convection. Vertical wind shear (BS06) was calculated by interpolation of winds to the height profile, taking the magnitude of the vector difference between surface and 6 km AGL. To compute storm-relative helicity (SRH03) we applied the internal dynamics method to estimate storm motions (Bunkers et al. 2000), then integrated between the surface and 3 km AGL. Temperature lapse rates (LR75) were computed between 500 and 700 hPa. A list of all parameters used in the study can be found in Table 1.

Definition of environmental proxies. The choice of environmental covariates to define thunderstorm, severe thunderstorm and tornadic thunderstorm situations was based on previously evaluated thresholds. For thunderstorms, a number of studies (Craven and Brooks 2004; van den Broeke et al. 2005; Kaltenböck et al. 2009; Westermayer et al. 2017; Taszarek et al. 2017, 2019) have compared unstable nonthunderstorm and thunderstorm environments and obtained a best discriminator in the range between 50 and 200 J kg^{-1}. For this study, a proxy of CAPE exceeding 150 J kg^{-1} was defined as meeting the conditions favorable for a thunderstorm, the same as in Taszarek et al. (2019, 2020).

A number of studies have demonstrated that the likelihood of severe convection increases along with increasing instability and increasing vertical wind shear that governs the organization and longevity of updrafts (Weisman and Klemp 1982; Brooks et al. 2003; Trapp et al. 2007; Allen et al. 2011; Brooks 2013; Púčik et al. 2015; Taszarek et al. 2017). For this reason, we used a composite product of CAPE and BS06 (WMAXSHEAR; a theoretical estimate of the updraft's vertical velocity multiplied by a vertical wind shear) for assessing the climatological aspects of severe thunderstorm environments. A threshold of WMAXSHEAR exceeding 500 $m^2 s^{-2}$ (with the assumption that BS06 should be no lower than 10 m s^{-1}) is used here to define a severe thunderstorm environment, based on results from prior work (Brooks et al. 2003; Allen et al. 2011; Brooks 2013; Púčik et al. 2015; Taszarek et al. 2017, 2019).

To define a potential tornadic thunderstorm we use a significant tornado parameter (STP) based on updated formula from Coffer et al. (2019), which consists of CAPE, lifted condensation level, SRH, effective shear and CIN. STP values of approximately 1 have been shown to be capable of discriminating between significant tornadic and nontornadic supercells over the

Table 1. List of parameters used in the study.

Abbreviation	Full name	Units
MIXR	0–500 m above ground level mixed-layer mixing ratio	g kg^{-1}
CAPE	0–500 m above ground level mixed-layer convective available potential energy	J kg^{-1}
CIN	0–500 m above ground level mixed-layer convective inhibition	J kg^{-1}
LR75	700–500 hPa temperature lapse rate	°C km^{-1}
T2M	2 m above ground level temperature	°C
BS06	0–6 km above ground level bulk wind difference (shear)	m s^{-1}
SRH03	0–3 km above ground level storm-relative helicity	$m^2 s^{-2}$
RH04	0–4 km above ground level mean relative humidity	%
WMAXSHEAR	A square root of 2 times CAPE multiplied by BS06 (Taszarek et al. 2017)	$m^2 s^{-2}$
STP	Significant tornado parameter (Coffer et al. 2019)	—
SCP	Supercell composite parameter (Gropp and Davenport 2018)	—
SHIP	Significant hail parameter (NOAA Storm Prediction Center)	—
CP	ERA5 1-h accumulated convective precipitation	mm h^{-1}

United States (Grams et al. 2012; Gensini and Bravo de Guenni 2019). However, over Europe this threshold is less effective in predicting significant tornadoes (Kaltenböck et al. 2009; Rodriguez and Bech 2018), as from a climatological perspective instability and helicity are typically lower compared to environments in the United States (Gensini and Ashley 2011; Taszarek et al. 2018). To account for this effect, in this study we apply a lowered STP threshold of 0.75 (for both domains) to define situations with potential tornadic thunderstorms. The formula for the supercell composite parameter (SCP) is taken from Gropp and Davenport (2018), while significant hail parameter (SHIP) is based on the original equation available in NOAA Storm Prediction Center (www.spc.noaa.gov).

Environmental proxies are only an imperfect conditional approximation of convective activity, as not every favorable environment produces a severe thunderstorm, or a thunderstorm at all. For this reason we add an additional condition using the convective precipitation (CP) hourly accumulation as a proxy for convective initiation. The underlying ERA5 convective parameterization (Bechtold et al. 2014) applies a mass flux closure scheme with entrainment that triggers convection based on either surface fluxes or synoptic motions, thereby providing greater confidence of initiation. We apply a CP threshold of 0.25 mm h^{-1}, following Taszarek et al. (2020) who used the same proxy to construct a climatology of thunderstorm environments with ERA5. Similar approaches have also been used in many prior studies using reanalyses and climate projections (Trapp et al. 2009; Tippett et al. 2012; Romps et al. 2014; Allen and Tippett 2015; Púčik et al. 2017; Tippett and Koshak 2018; Taszarek et al. 2019; Tippett et al. 2019). The CP proxy in this study is applied by taking into account hourly precipitation accumulation for the hour following instantaneous characterization of environmental parameters (i.e., CAPE threshold from 1700 UTC is matched with CP for 1700–1800 UTC). A summary of applied conditional proxies is presented in Table 2. Since the majority of above described proxies have been developed for convective events occurring over land, in this study we do not evaluate modeled (severe) thunderstorm and tornadic environments over the sea and ocean surface.

As demonstrated by Tippett et al. (2019) performance of thunderstorm proxies vary by the region and time of the year. This poses challenges, particularly given how different convective environments are between the United States and Europe. Thus, such an analysis will be always burdened with some degree of inaccuracy, no matter the parameter chosen. Application of convective proxies obviously does not provide an explicit number of storm events (Hoogewind et al. 2017), but it helps to narrow situations to those that may most likely result in (severe) thunderstorms. Evaluation of long-term changes in such environments should be representative of relative changes in the frequency of actual convective events, even though magnitude of these changes may not be in a perfect agreement.

Results

Ingredients for deep moist convection. Consistent with the recent reports of the Intergovernmental Panel on Climate Change (IPCC 2018), statistically significant upward trends are found in the upper distribution of surface temperature (T2M; Fig. 1a) over the last four decades for the majority of Europe (>0.75°C $decade^{-1}$). In contrast, over the United States

Table 2. Environmental proxies for thunderstorm, severe thunderstorm, and tornadic thunderstorm environments.

Category	Proxies
Thunderstorm	CAPE > 150 J kg^{-1}, CP > 0.25 mm h^{-1}
Severe thunderstorm	CAPE > 150 J kg^{-1}, CP > 0.25 mm h^{-1}, BS06 > 10 m s^{-1}, WMAXSHEAR > 500 m^2 s^{-2}
Tornadic thunderstorm	CAPE > 150 J kg^{-1}, CP > 0.25 mm h^{-1}, STP > 0.75

this trend is limited mainly to the high elevation mountain west. Temperature lapse rates between 700 and 500 hPa (LR75: Fig. 1b) describe the vertical gradients in the midatmosphere, and values exceeding 6.5°C km^{-1} can be linked to environments promoting severe thunderstorms (Brooks et al. 2003; Banacos and Ekster 2010; Taszarek et al. 2017). While the spatial climatology of LR75 is distinct from T2M, increasing trends in surface temperatures and reductions in low-level moisture are driving greater dry static stability over high terrain, and thus may lead to increasingly steep vertical gradients of temperature. These changes result in orographically correlated increases in LR75 over the western United States and parts of the Great Plains (>0.1°C decade^{-1}), particularly during spring and summer (seasonal changes of LR75 and T2M are available in the online supplementary material; https://doi.org/10.1175/BAMS-D-20-0004.2). Over Europe significant increases occur mainly over eastern part of the continent, especially around the Black Sea (>0.05°C decade^{-1}). This pattern may be related to small changes in near surface moisture [mixing ratio (MIXR); Fig. 1c], which along with increasing temperature leads to reduced relative humidity, and increasingly deep boundary layer mixing (Byrne and O'Gorman 2016). Similarly, over the mountainous west United States, negative trends in low-level moisture feedback to the generation of dry adiabatic lapse rates suggesting intensification of the process in which an elevated mixed layer (EML;

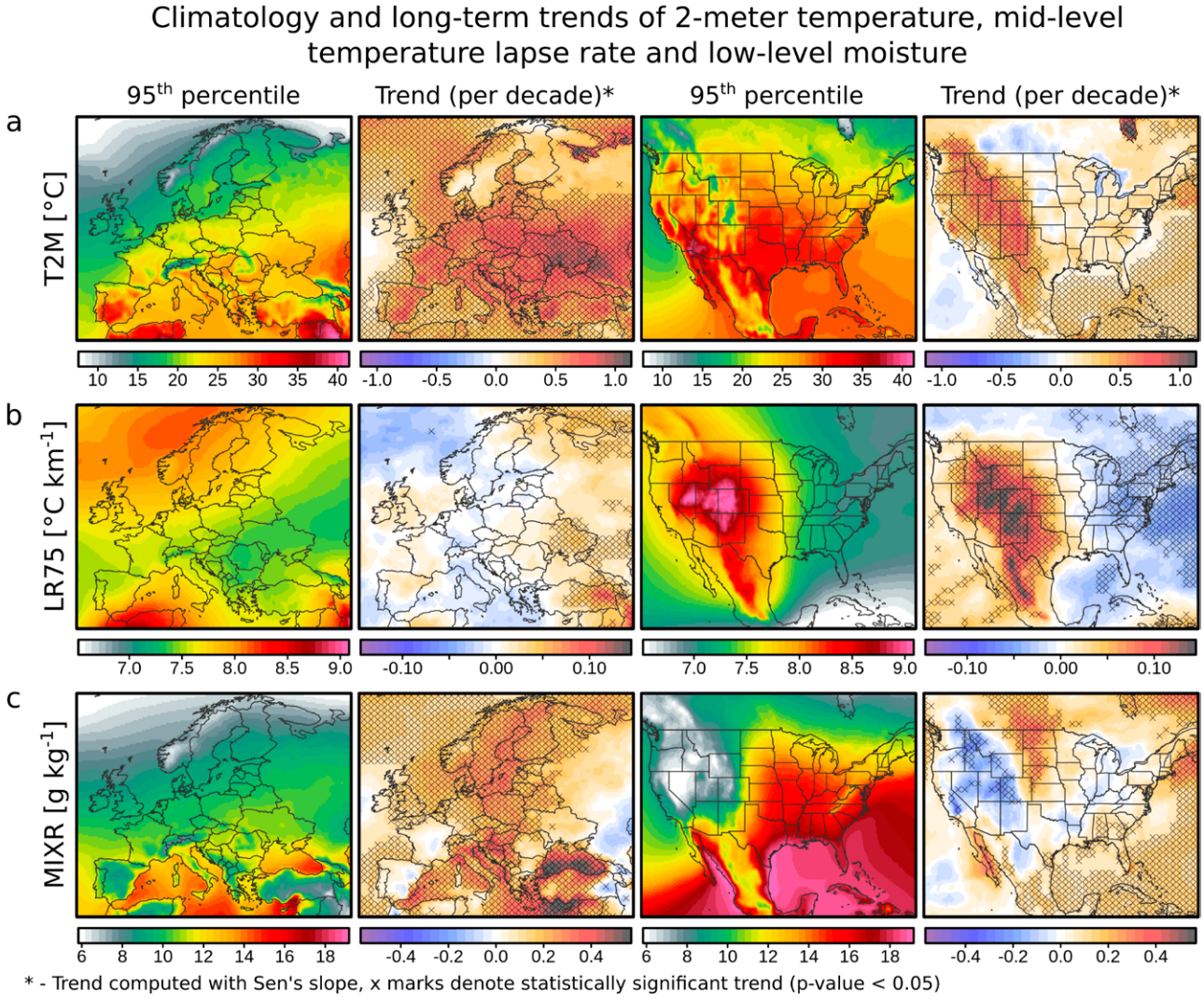

Fig. 1. (first column),(third column) A 41-yr climatology of (a) the 95th percentile of surface temperature (T2M), (b) midlevel temperature lapse rate (LR75), and (c) low-level moisture (MIXR) for Europe and the United States. (second column),(fourth column) Long-term trends are derived from annual values in hourly resolution and corresponding Sen's slope (values denote change per decade).

Carlson and Ludlam 1968) is generated. MIXR has increased substantially over northern and central Europe (0.2–0.3 g kg^{-1} decade^{-1}; Fig. 1c), while greater increases have occurred across the Mediterranean and Black Sea (>0.4 g kg^{-1} decade^{-1}), particularly during summer and autumn (appendix A). Over the United States increases are confined predominantly to the northern Great Plains (0.2 g kg^{-1} decade^{-1}), but on a seasonal basis large wintertime increases have been observed over the Southeast (0.4 g kg^{-1} decade^{-1}).

Combining the components from Fig. 1 we consider trends in vertically integrated thermodynamic instability using CAPE (Fig. 2a). Increases in CAPE are well correlated

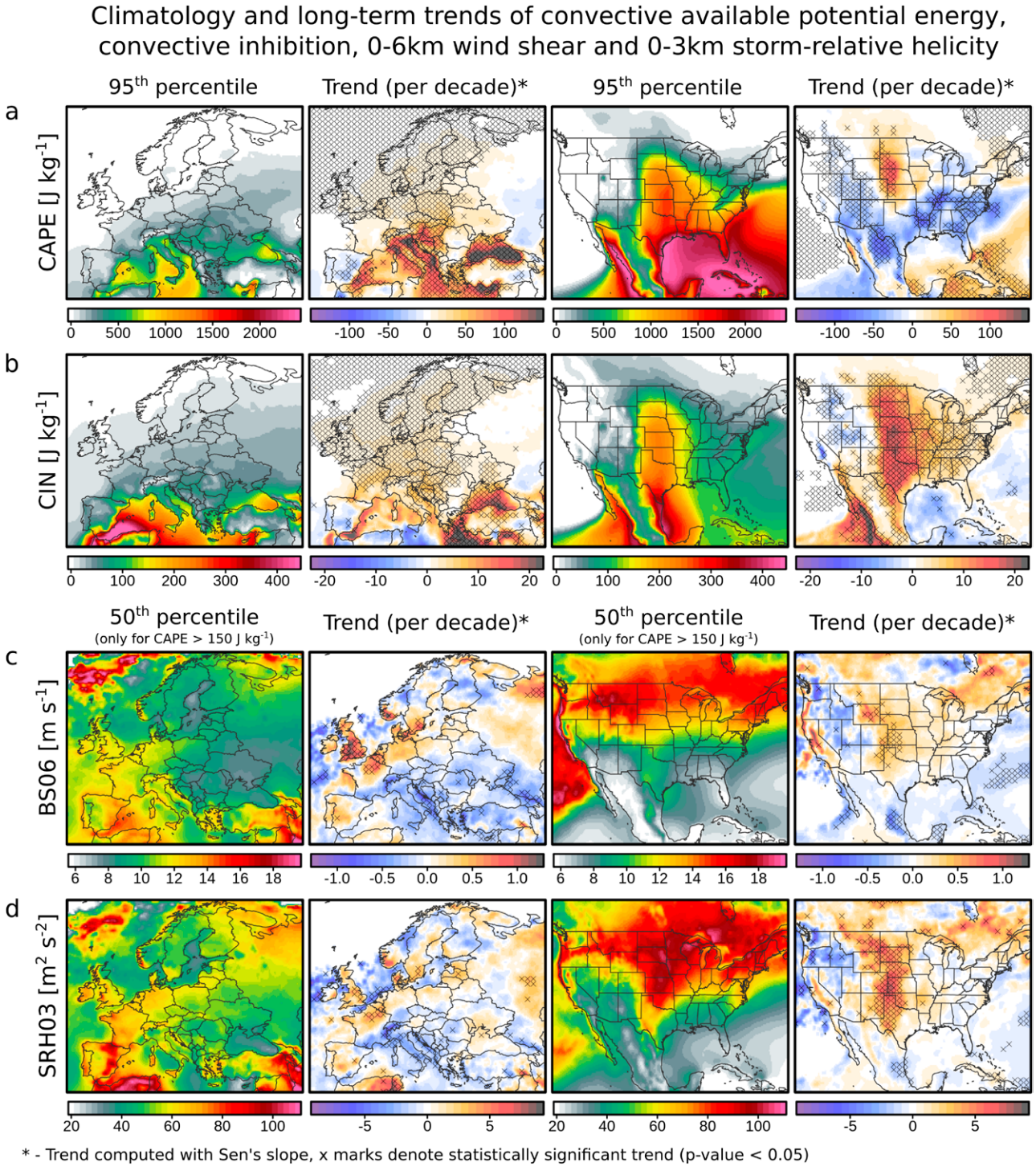

Fig. 2. As in Fig. 1, but for the 95th percentile of (a) convective available potential energy (CAPE), (b) absolute value of convective inhibition (CIN), and (c) 50th percentile of vertical wind shear (BS06) and (d) storm-relative helicity (SRH03). For BS06 and SRH03 only situations with CAPE > 150 J kg^{-1} are considered.

with rising MIXR (Fig. 1c) and indicate significant positive trends over northern and central Europe (25–50 J kg^{-1} $decade^{-1}$) with substantial increases over the Black Sea, northern Italy, and parts of the Mediterranean (>100 J kg^{-1} $decade^{-1}$). While the greatest changes in instability were detected over the northern Great Plains of the United States (>75 J kg^{-1} $decade^{-1}$), there are widespread robust negative trends of more than −50 J kg^{-1} $decade^{-1}$ over the majority of the continent. Changes in CAPE are spatially collocated with seasonal changes in MIXR and indicate increases over the Midwest during spring, the northern Great Plains during summer, and the Southeast during winter (contrasting decreases in summer and autumn; appendix B). Over Europe significant decreases in CAPE are found over the Iberian Peninsula.

However, the presence of instability itself is not sufficient for the formation of thunderstorms, as convective initiation is necessary to benefit from the availability of CAPE. This process may be inhibited if stable layers with negative parcel buoyancy occur in the lowest portions of the troposphere. Increases in CIN over Europe are generally modest (5–15 J kg^{-1} $decade^{-1}$) and spatially collocated with increasing CAPE (Fig. 2b). The largest trends, exceeding 20 J kg^{-1} $decade^{-1}$, occur over eastern portions of the Mediterranean and Black Sea seasonally tied to summer (appendix C). Robust increases in CIN occur over the majority of the United States, particularly over the Great Plains (>15 J kg^{-1} $decade^{-1}$), including areas where the underlying trend in CAPE has also shown decreases (Fig. 2b). On a seasonal basis the highest significant increases have occurred over the southern Great Plains during spring (>30 J kg^{-1} $decade^{-1}$). Substantial changes in CIN can be partially explained by the robust increases in LR75 over western mountainous regions (Fig. 1b) and subsequent advection of an EML over the lower elevations of the continent (especially the southern and central Great Plains). This process may lead to a more stable stratification between the boundary layer and the EML, and hence stronger CIN as a result. Substantial increases in CIN suggest that convective initiation may be delayed within the diurnal cycle, precluded in totality, or lead to explosive convective initiation with severe weather when instability is allowed to reach its diurnal peak (Trapp and Hoogewind 2016; Hoogewind et al. 2017; Rasmussen et al. 2020).

Vertical wind shear is an important component related to storm severity (Brooks et al. 2003; Allen et al. 2011; Brooks 2013; Púčik et al. 2015; Taszarek et al. 2017) and can be vectorized by a difference of wind speed and direction between the surface and a height of 6 km (BS06; Fig. 2c) or by changes in the speed and direction of the vertical wind profile up to 3 km (SRH03; Fig. 2d). Long-term changes in the median of BS06 and SRH03 conditional on CAPE > 150 J kg^{-1} indicate negative trends over portions of southern and southeastern Europe (–0.5 m s^{-1} $decade^{-1}$). This contrasts with significant increases over northwestern Europe (0.75–1.25 m s^{-1} $decade^{-1}$), seasonally tied mainly to the summer (appendix D). These changes may be driven by shifts and/or weakening in the jet stream (Archer and Caldeira 2008; Pena-Ortiz et al. 2013) as a result of decreasing horizontal temperature gradient between the midlatitudes and the Arctic (Coumou et al. 2015). Over the United States a modest change in BS06 (0.4 m s^{-1} $decade^{-1}$) and a significant increase of SRH03 (6 m^2 s^{-2} $decade^{-1}$) is found over the Great Plains, partially collocated with increasing CAPE. Seasonally, these increases take place mainly during spring and summer (appendix E). A possible explanation for a change in SRH03 may be related to strengthening of the Great Plains low-level jet that was noted over a historical period (Barandiaran et al. 2013) and is an expected outcome of a warming climate (Cooke et al. 2008; Tang et al. 2017).

Seasonal variability of severe thunderstorm environments. Combining CAPE and BS06 into a bivariate proxy (Brooks et al. 2003) of conditions favorable to severe thunderstorms, trends in the seasonal distribution of the WMAXSHEAR product (Del Genio et al. 2007; Brooks 2013; Taszarek et al. 2017, 2018, 2019) were considered (Fig. 3). Climatology of WMAXSHEAR over Europe indicates that severe thunderstorms are most likely to occur during summer in the corridor

from northeastern Spain through portions of central Europe, Italy, and the Balkan Peninsula. The strongest long-term increases in that period are observed over northwestern, northern, central and parts of southern Europe, with localized decreases over the Iberian Peninsula, Balkan Peninsula, and far eastern Europe, consistent with changes in MIXR (Fig. 1c). Increases during autumn are more closely related to sources of moisture, with changes proximal to the Mediterranean, Black Sea, and North Sea. Little to no trend is found during the winter, which is also a period of climatologically low WMAXSHEAR. During spring there are positive trends for

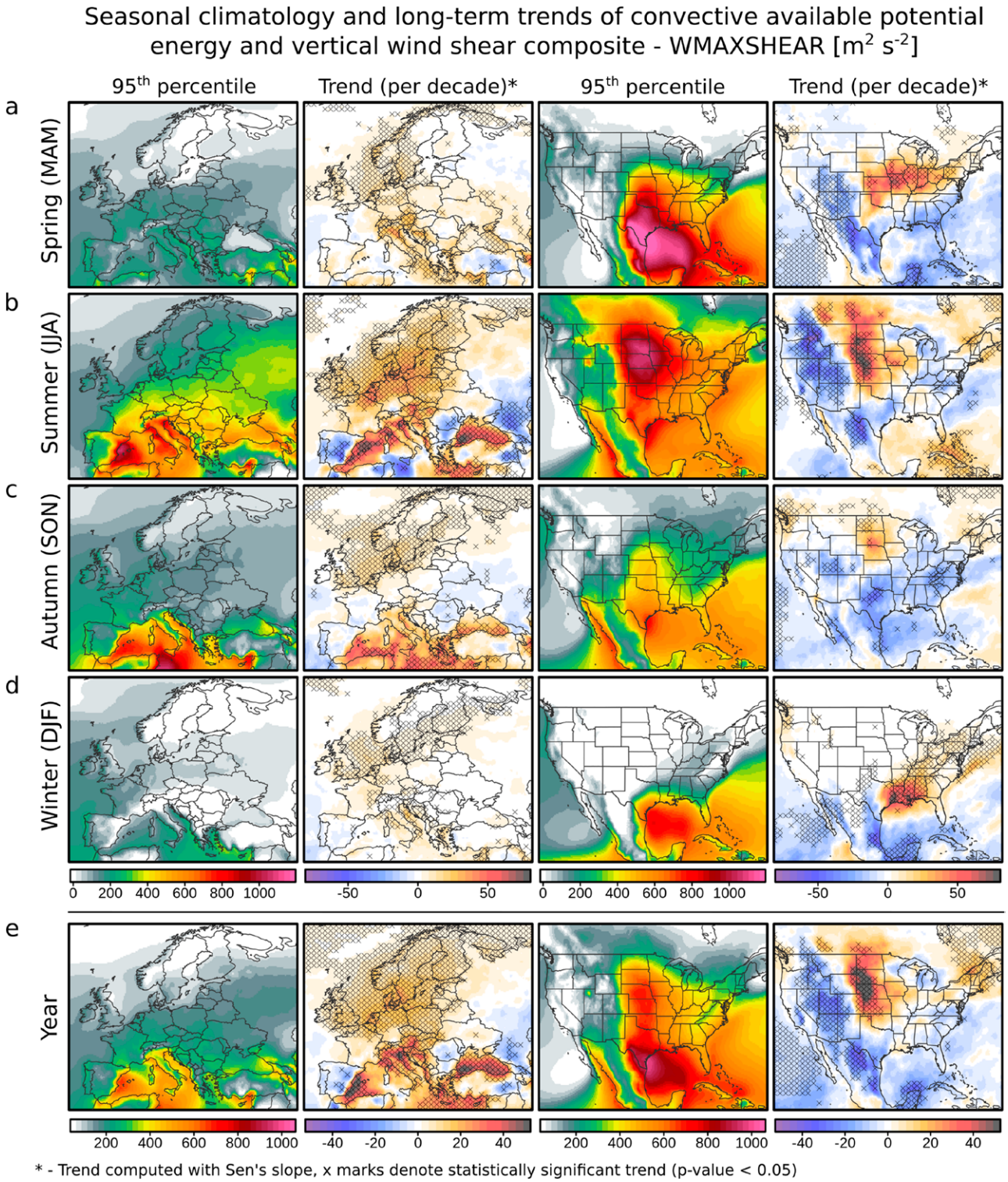

Fig. 3. As in Fig. 1, but for the convective available potential energy and vertical wind shear composite (WMAXSHEAR) by season [(a) spring, (b) summer, (c) autumn, and (d) winter] and (e) for the whole year.

portions of northwestern, central, and southern Europe, suggesting spring is an increasingly active severe thunderstorm season. These changes are driven mainly by significant increases to MIXR and CAPE, and hence potential updraft intensity, despite modest changes to BS06.

Over the United States the spatial pattern in severe convection has greater variability in response to the seasonal cycle, shifting from the southeastern United States in the winter northward toward the Great Plains in spring and summer (Fig. 3). Consistent with changes in MIXR, during spring there is a significant increase of WMAXSHEAR over the Midwest. During summer a robust increase is observed over the northern Great Plains, which is a result of positive trends in both CAPE and BS06. This signal persists in autumn but is generally weaker, and is counterbalanced by modest decreases over the southern Great Plains and the Southeast. Despite climatologically low WMAXSHEAR during winter, robust trends of over 50 $m^2 s^{-2}$ $decade^{-1}$ are found over the Southeast, suggesting increasing potential for severe thunderstorms including tornadoes. These winter patterns are mainly driven by rising MIXR, T2M, and resulting CAPE, rather than modulations in BS06. As illustrated by Molina and Allen (2020) these changes are induced by increases in advective moisture fluxes from the Gulf of Mexico.

An evaluation of composite parameters used in the operational forecasting of severe thunderstorms (Fig. 4) indicate increases in extreme convective environments for even broader areas across the United States. Tail distributions (99.9th percentile) of SCP and SHIP feature positive trends over the Great Plains, Midwest, and portions of the Southeast (seasonally consistent with WMAXSHEAR), but not all of the trends in these areas are significant or spatially cohesive. Increases over the Midwest are partially consistent with Tang et al. (2019) for changes in large hail environments based on NARR. Extremes of STP (Fig. 4c) feature slightly different spatial patterns with climatological peaks occurring over portions of the southern Great Plains and the Southeast. Significant increasing trends are observed over the Southeast and are explicitly tied to spring and winter (appendix F), which is in agreement with Gensini and Brooks (2018).

Over Europe, there are positive increases to SCP, SHIP, and STP over the northwest, central, and south, along with minor decreases over the east that are broadly consistent with changes to WMAXSHEAR (Figs. 3 and 4). However, climatologically these parameters reach much lower values over Europe compared to the United States (where SCP, SHIP, and STP were originally developed), and the rate of change is also much smaller. Compared to tornado reports presented in Groenemeijer et al. (2017) and Taszarek et al. (2019), our modeled tornadic thunderstorm environments likely underestimate frequencies for the northwest, and overestimate over the southwest of Europe. However, these differences may be a result of reporting biases with more cases of weak and short-lived tornadoes reported over densely populated areas such as Benelux. The increased climatological number of tornado environments over western Russia is consistent with tornado reports evaluated by Chernokulsky et al. (2020).

Importance of convective inhibition and initiation. A factor that has not been widely considered in analyzing historical trends in severe thunderstorms is CIN. This is partly driven by the lower vertical resolution of reanalysis in earlier studies as compared to the dataset applied here, which allows for better detection of CIN. Here we consider the fraction of environments that may inhibit convection (absolute CIN > 75 J kg^{-1}; Bunkers et al. 2010; Gensini and Ashley 2011; Westermayer et al. 2017; Taszarek et al. 2019) conditional on all potential thunderstorm environments (CAPE > 150 J kg^{-1}). Long-term trends of this parameter feature significant increases over eastern Europe (2%–3% $decade^{-1}$; Fig. 5a). However, climatologically, CIN has generally low values across Europe, and hence changes reflect relatively small differences (Fig. 2b). Over the United States where CIN is typically much higher, a robust increase in environments that inhibit convection (3%–5% $decade^{-1}$) has taken place over almost the entire country. Similar results regarding spatial patterns were obtained when applying a CIN threshold of 50, 100, and 150 J kg^{-1} (online supplementary material).

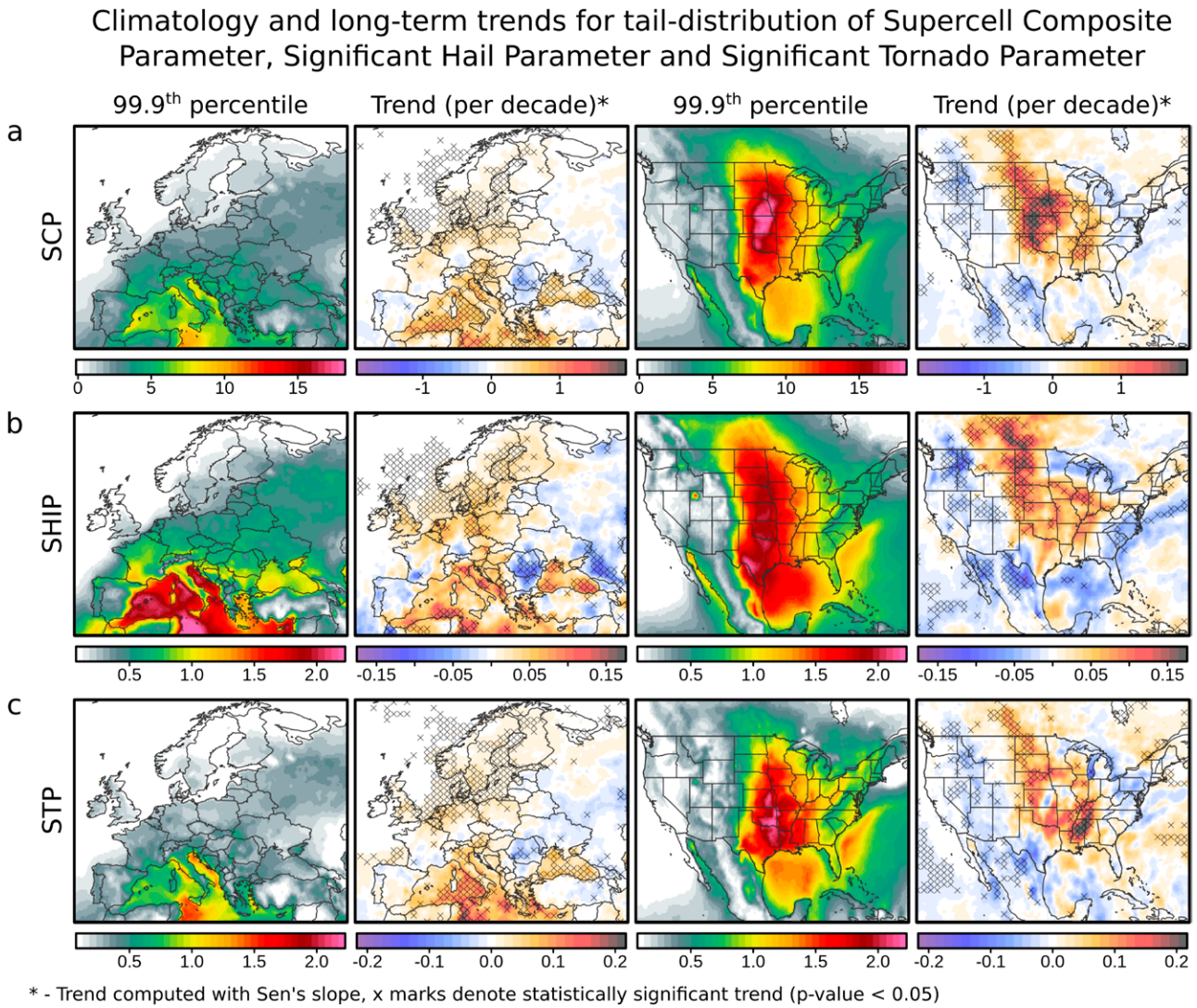

Fig. 4. As in Fig. 1, but for the 99.9th percentile of (a) supercell composite parameter (SCP), (b) significant hail parameter (SHIP), and (c) significant tornado parameter (STP).

Changes in inhibition can be a limiting factor to the increase in the number of thunderstorms resulting from the more frequent unstable environments. To confirm this result, we consider the modeled convective precipitation variable as a proxy for convective initiation (Fig. 5b), using the fraction of unstable environments that simultaneously are associated with precipitating situations (Brooks 2009; Groenemeijer et al. 2017). There has been a significant decrease in the fraction of thunderstorm environments resulting in precipitation that is partly coincident with areas of increasing convective inhibition. Over western and northern Europe, the decreasing fraction of precipitating environments does not appear to be related to significant changes in CIN fractions, which can be explained by overall weak inhibition (CIN > 75 J kg^{-1} is rare over these regions). However, the "efficiency" of convective environments may be also explained by long-term changes in the frequency of cyclones (Sepp et al. 2005; Parding et al. 2019), which over northwestern Europe are an important trigger for convection. These systems provide strong synoptic-scale lift, and drive the progress of atmospheric fronts that are often associated with deep moist convection (van Delden 2001; Kolendowicz 2012; Wapler and James 2015; Piper et al. 2019). The relative scale of these changes to initiating environments are also important. For example, a few percent per decade over the British Isles is a small fractional change relative to climatology (20%–40%). In contrast, over the Great Plains the climatological mean efficiency is 5%–10%, and thus a change of 1%–2% represents a more significant reduction.

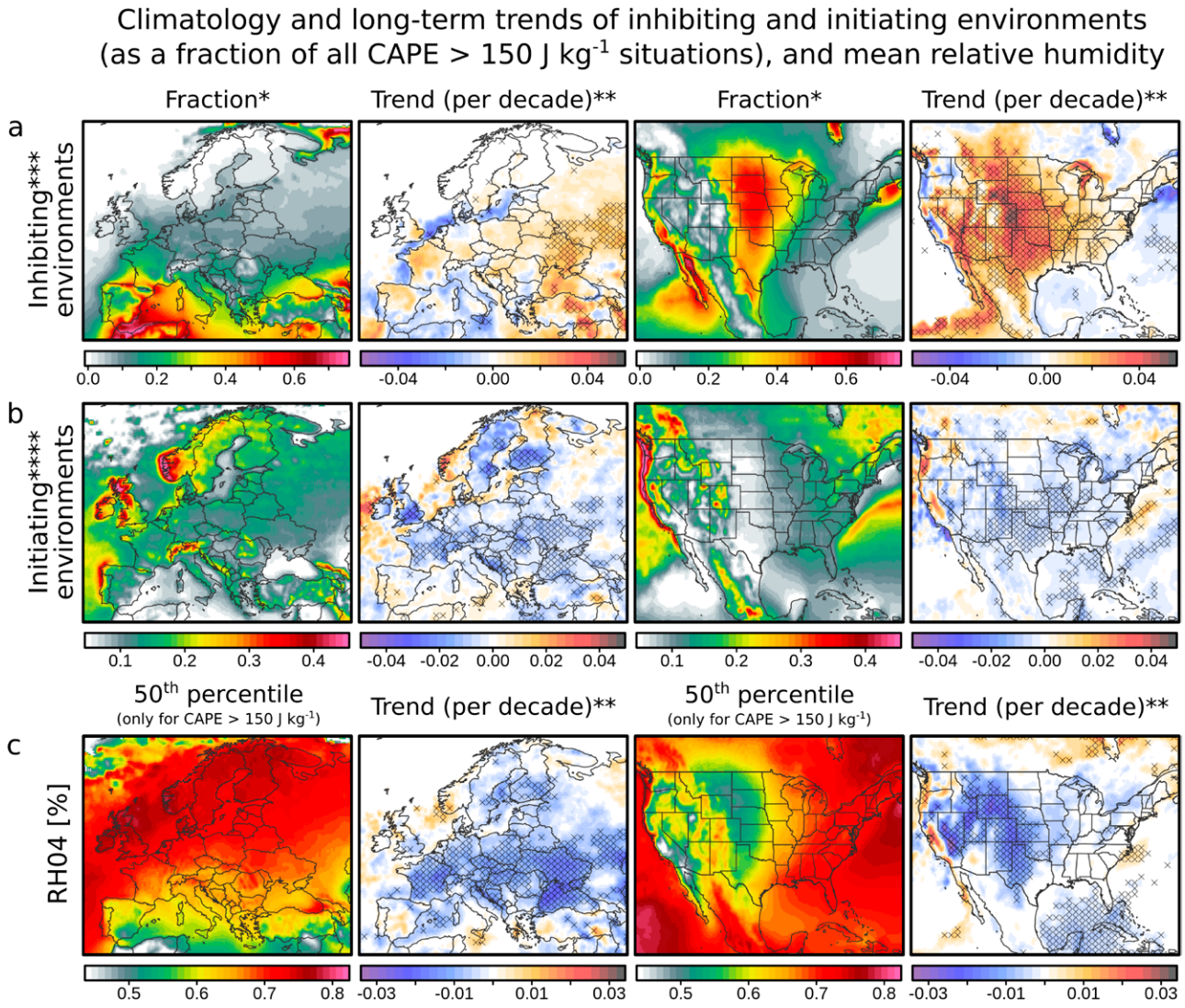

* - Fraction is denoted by situations with inhibiting (a) or initiating (b) environments among cases when CAPE > 150 J kg^{-1}
** - Trend computed with Sen's slope, x marks denote statistically significant trend (p-value < 0.05)
*** - Inhibiting environment is considered when absolute CIN > 75 J kg^{-1}
**** - Initiating environment is considered when CP > 0.25 mm h^{-1}

Fig. 5. As in Fig. 1, but for the fraction of (a) inhibiting and (b) initiating environments (relative to all CAPE > 150 J kg^{-1} situations), and for the 50th percentile of (c) mean 0–4 km relative humidity (RH04) only for situations with CAPE > 150 J kg^{-1}.

Another relevant factor is changes in the mean relative humidity (RH04; Fig. 5c). A robust decrease of around 2%–3% decade^{-1} in the median is observed over the majority of Europe and portions of western and central United States, partially intersecting increases in CIN (Fig. 2b). According to Westermayer et al. (2017), decreasing low and midlevel relative humidity and resulting dry-air entrainment into a developing updraft may lead to reductions in thunderstorm initiation despite availability of ample CAPE. This process may be partially responsible for decreases in initiating environments that are observed over Europe, and are not related to changes in CIN. While this hypothesis has not been tested over the United States, it offers a potential direction of future exploration. Pronounced decreases in land surface relative humidity are also relevant to a warming climate, as indicated by Byrne and O'Gorman (2016).

Changes in the frequency of modeled thunderstorms. To empirically estimate how the frequency of thunderstorms has changed since 1979 we combine changes to convective

initiation with proxies for environments favorable to thunderstorms, severe thunderstorms, and tornadic thunderstorms (Table 2, Figs. 6 and 7). Consistent with rising instability, there is an increase in the number of (severe) thunderstorm environments over northwestern, central, and southern Europe, which partly contrasts the decrease to the overall fraction of precipitating environments. This suggests that while a lower fraction of environments results in convective precipitation, there is a considerable increase in the number of periods with conditions favorable to (severe) thunderstorms, which is also an expected outcome of the projected future European climate (Rädler et al. 2019). This change is most pronounced over Italy, contrasting smaller decreases over eastern Europe that result from an increasing fraction of inhibiting environments (Fig. 5a) and decreases in relative humidity (Fig. 5c). Decreases over the Iberian Peninsula are primarily associated with reductions in instability (Fig. 2a). Positive trends in tornadic thunderstorms, which are relatively rare over Europe, are more restricted and mainly confined to the western Turkish coast and Italy.

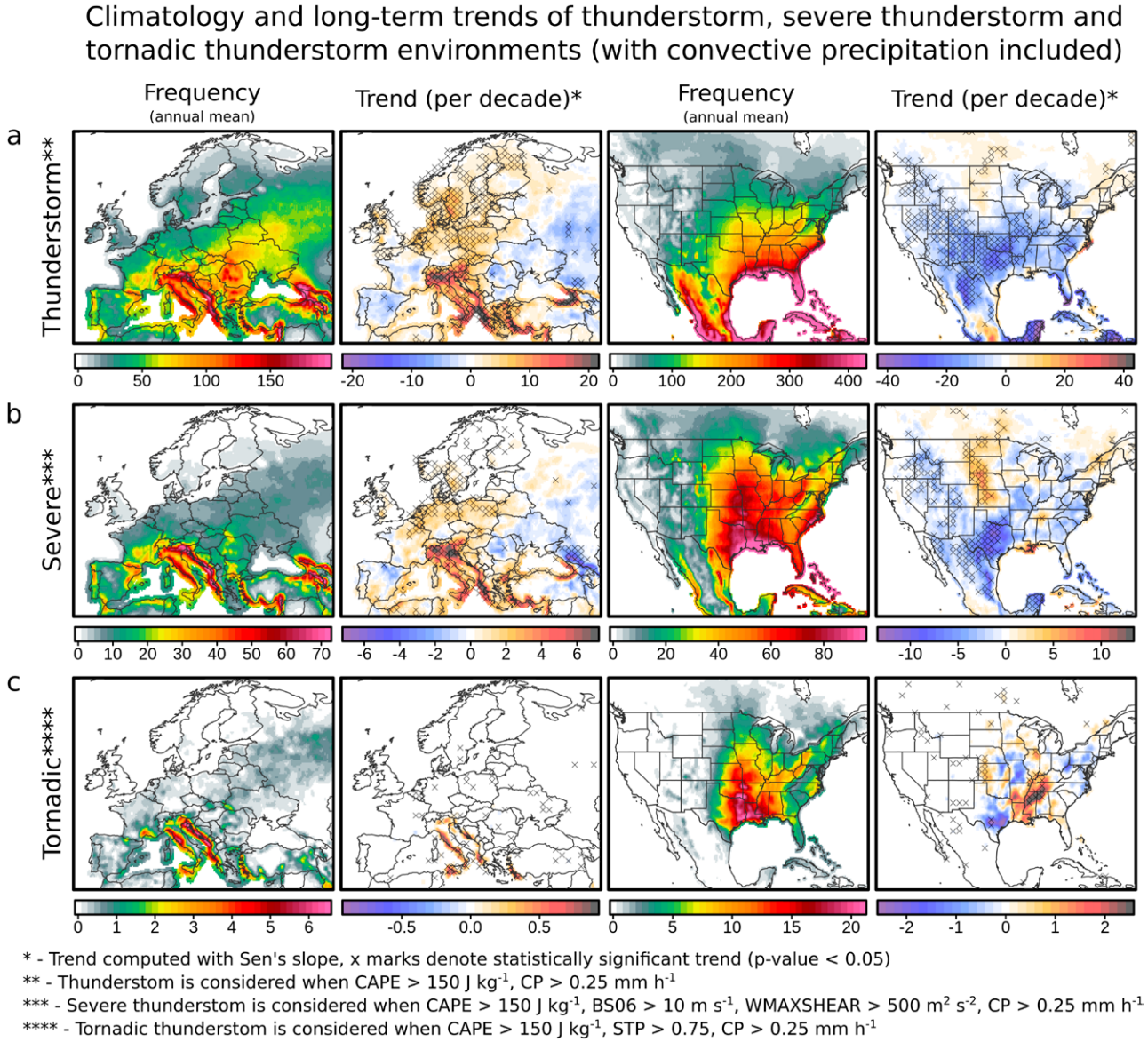

Fig. 6. As in Fig. 1, but for the frequency (h) of (a) thunderstorm, (b) severe thunderstorm, and (c) tornadic thunderstorm environments (with convective initiation included). Please note that color bar ranges differ between Europe and the United States. Modification of this figure where convective precipitation proxy is excluded is available in the online supplementary material.

Over the United States there is a robust negative trend for both thunderstorm and severe thunderstorm environments over the majority of southern and western parts of the country. Despite robust increases to favorable environments over the Great Plains and Midwest (Figs. 3 and 4, appendix B), there is no increase in the frequency of thunderstorm environments conditional on initiation (Fig. 6a). Instead, there is only a slight increase in severe thunderstorms over portions of the northern Great Plains (Fig. 6b). Regional changes indicate

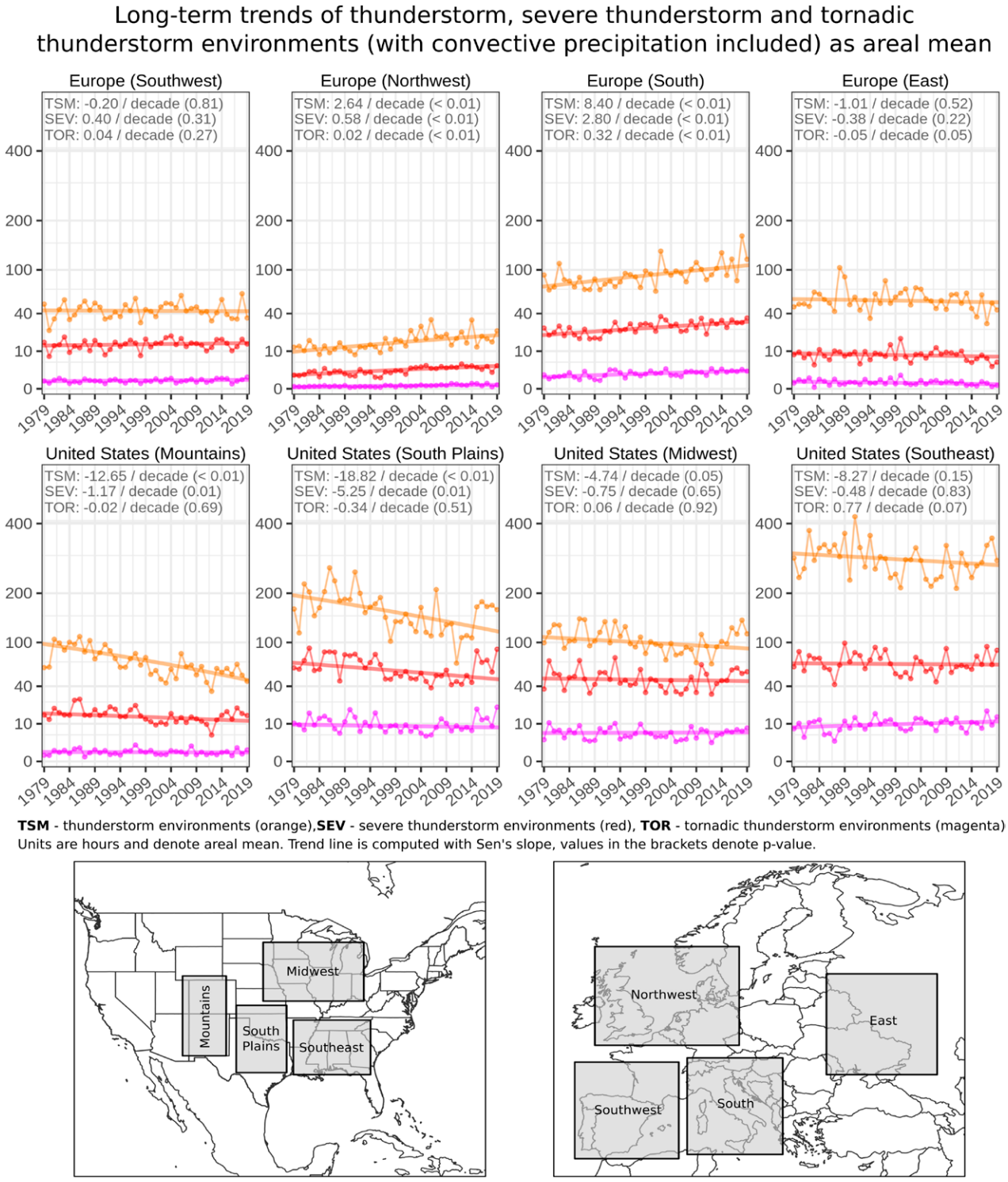

Fig. 7. Long-term trends in the frequency (h) of thunderstorm (TSM; orange), severe thunderstorm (SEV; red), and tornadic thunderstorm environments (TOR; magenta) derived as areal mean from selected regions. Values at the top of each chart indicate Sen's slope (values denote change per decade) and the *p* value is in parentheses. Please note that values on the *x* axis are presented in a square-root scale.

decreasing trends over the southern Great Plains, mountains, and Midwest with mean rates of −18.8, −12.7, and −4.7 h with thunderstorms per decade, respectively (Fig. 7). In contrast, there are increases over northwestern and southern Europe (2.6 and 8.4 h decade^{-1}, respectively; Fig. 7). Considering instead a trend in days (with at least one favorable environment), the spatial patterns and the fractional magnitude of the difference is very similar to hourly estimates over both continents (not shown).

Cross validating changes in thunderstorm hours over the United States with convective frequency based on CG lightning data for 1989–2018, there is a similar spatial pattern with the biggest decreases observed during the summer and smaller during spring and autumn over the southern Great Plains (Fig. 8). This result supports the ability of reanalysis-derived trends

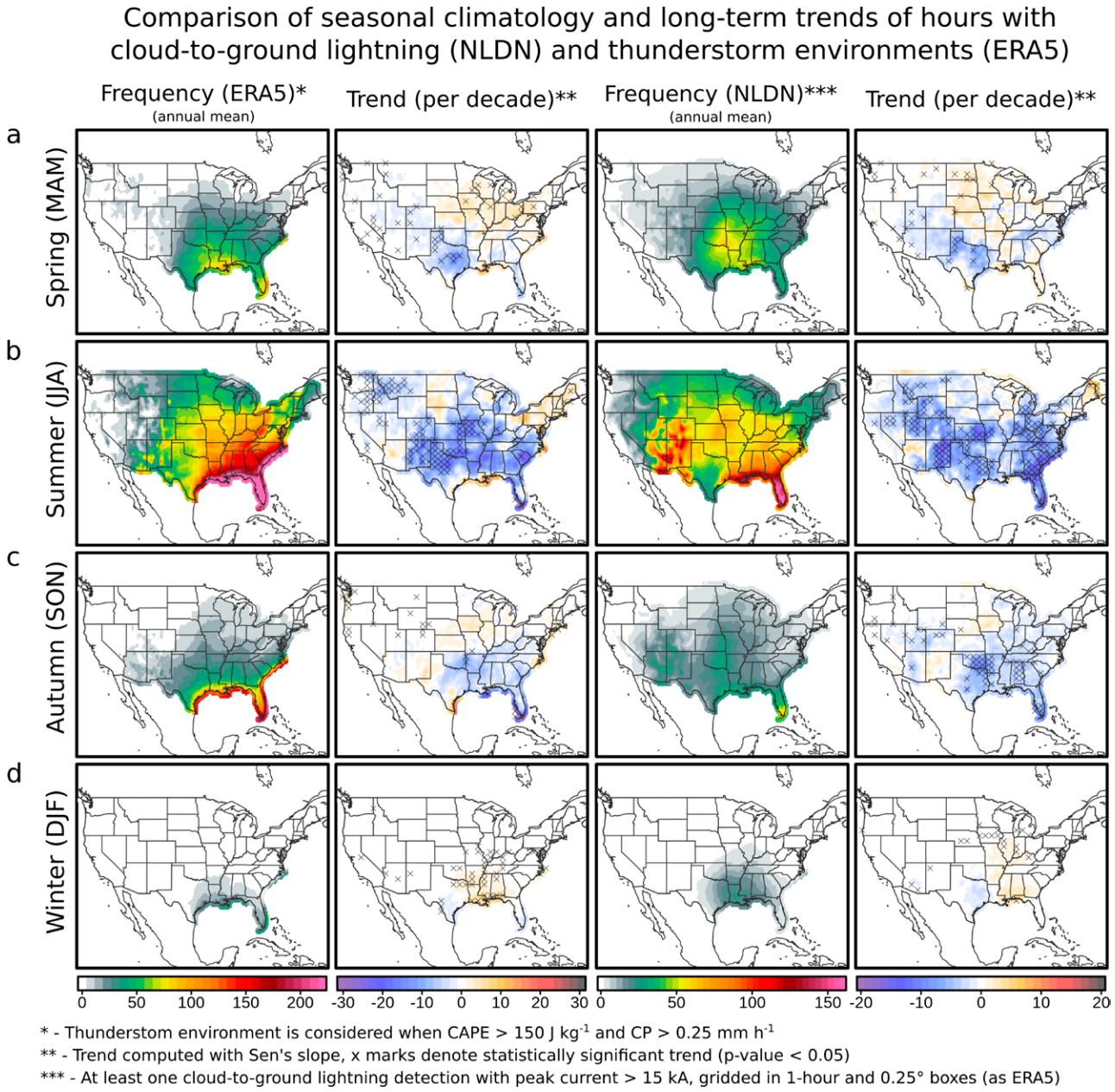

Fig. 8. (first column),(third columns) A 30-yr (1989–2018) climatology of the number of hours with potential thunderstorm environments and cloud-to-ground lightning from National Lightning Detection Network (NLDN) for the United States by season: (a) spring, (b) summer, (c) autumn, and (d) winter. (second column),(fourth columns) Long-term trends are derived by seasonal values in hourly resolution and corresponding Sen's slope (values denote change per decade). Please note that color bar ranges differ between two methods.

in convective environments to reproduce changes in observational data, and is suggestive that thunderstorms have become less frequent over the last few decades. However, we note that proxies applied in this study tend to overestimate thunderstorm frequency during summer, and along the coastline. Conversely, underestimation is observed during winter and over the mountains (Fig. 8). This results is consistent with Tippett et al. (2019) that performance of thunderstorm proxies typically vary by region and time of the year.

For tornadic storms, there is a shift in the spatial frequency of environments toward the Southeast that is in agreement with the results obtained by Gensini and Brooks (2018). Consistent with patterns obtained for the 99.9th percentile of STP (Fig. 4c, appendix F), the highest increases in the frequency of tornadic thunderstorm environments are observed during spring and winter. However, when an areal mean is considered for the Southeast (Fig. 7), trends in tornadic thunderstorms are insignificant (p value of 0.07). Conversely, significant positive trends in tornadic environments are observed over southern Europe, but they are very small (0.3 h decade^{-1}; Fig. 7).

Finally we assess trends for southeastern Oklahoma and northeastern Italy (Fig. 9), two locations characterized by similarly high frequencies of severe convective storms (Smith et al. 2012; Taszarek et al. 2019), but representative of the differences in historical trends between Europe and the United States. Decreasing CAPE over southeastern Oklahoma contrasts with substantial increases over northeastern Italy. In both cases the changes in CAPE occur mainly during the summer (a median change of ~200 J kg^{-1} over both locations considering the difference between 1979–88 and 2009–19; Fig. 9a). However, there are significant increases to CIN throughout the whole distribution over Oklahoma, which causes a reduction in the frequency of initiating environments. Over Italy there is little change to CIN, resulting in a rising frequency of thunderstorms as a result of substantial increases to instability (Fig. 8c). This further reinforces that changes to convective environments are less representative without the context provided by the variations in CIN, and the resulting likelihood of convective initiation. These results imply that further increases to CIN induced by a globally warming climate, may have more significant implications for the future frequency of severe thunderstorms than is currently expected (Diffenbaugh et al. 2013; Trapp and Hoogewind 2016; Hoogewind et al. 2017; Rädler et al. 2019; Chen et al. 2020).

Discussion and concluding remarks

Historical changes to the frequency and incidence of convection have long proven elusive to identify. Here we show that changes in favorable convective environments derived from reanalysis data are only partially consistent with the expectations for both continents under a warming climate [e.g., different outcomes regarding changes in BS06 as compared to Hoogewind et al. (2017), Rädler et al. (2019) or decreases in CAPE over the southeastern United States during summer]. The factor that drives the increase in convective environments is predominantly thermodynamic instability tied to more readily available low-level moisture, in agreement with future projections over the northern Great Plains (Diffenbaugh et al. 2013; Hoogewind et al. 2017; Chen et al. 2020) and the majority of Europe (Púčik et al. 2017; Rädler et al. 2019). However, this does not necessarily translate to an increase in the frequency of thunderstorms.

Whether convection initiates is a substantial contribution to the resulting changes in thunderstorms. The expected increases from growing thermodynamic favorability are limited by decreasing fraction of initiating environments. While increases in convective environments are present over parts of the Great Plains and Midwest, these are partially offset by the reductions in the frequency of convective initiation events. The increases to CIN in the United States over the past four decades are substantial, and occur throughout

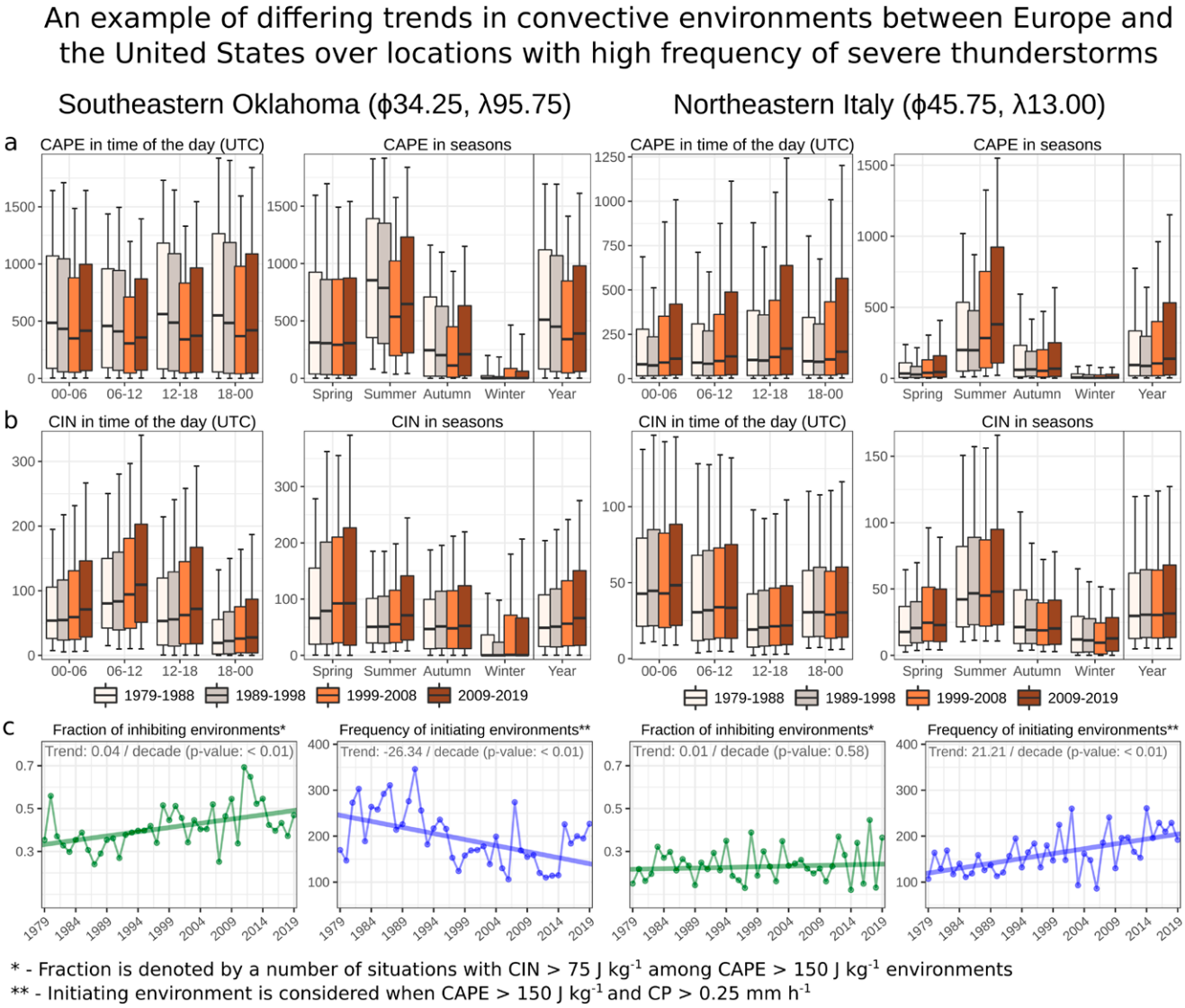

Fig. 9. Box-and-whisker plots (the median is denoted as a horizontal line inside the box, the edges of the box represent the 25th and 75th percentiles, and whiskers represent the 10th and 90th percentiles) representing diurnal and seasonal cycle of (a) CAPE (J kg^{-1}) and (b) CIN (J kg^{-1}) over southeastern Oklahoma and northeastern Italy (limited to situations with CAPE > 0 J kg^{-1}). (c) Fraction of inhibiting environments (as in Fig. 4a) and the frequency of unstable and initiating environments (as in Fig. 5a) over particular years. Trend lines are derived from Sen's slope.

the whole parameter distribution. In Europe, thermodynamic parameters become more favorable over the southern, central, and northern parts of the continent during spring, summer, and fall, but increases in CIN and reductions in relative humidity partially offset these gains. Changes to conditional BS06 and SRH03 play a reduced role in contributing to convective environments, with most of trends being insignificant. Modest significant increases have been observed over northwestern Europe and the Great Plains. This indicates that trends in the severe thunderstorm environments over the last decades have been mostly driven by changes in instability, and factors leading to convective initiation, rather than modulations in the wind profile.

As both observational and radar-based approaches to estimate convective frequency are limited in their spatiotemporal coverage and consistency, whether trends presented in this study are manifesting in observations can be challenging to quantify (Brooks et al. 2014; Allen and Tippett 2015; Edwards et al. 2018; Gensini and Brooks 2018; Allen 2018; Tang et al. 2019). This is because trends driven by the physical processes are difficult to

separate from temporal and spatial biases arising from increased severe weather reporting that has taken place over the recent years (Mahoney 2020). This problem strongly influences European severe weather observational data, as noted by Groenemeijer et al. (2017) and Taszarek et al. (2019). Nonetheless, our results are consistent with prior European studies considering historical trends in convective environments using numerical weather prediction data that offer a more consistent record both spatially and temporally (Pistotnik et al. 2016; Rädler et al. 2018; Taszarek et al. 2019).

Implications for the change to convective environments stretch beyond those for severe thunderstorms as well. Convective precipitation plays a substantive role in the hydroclimate of both Europe and the United States, particularly in the spring and summer (Punkka and Bister 2005; Chernokulsky et al. 2019; Haberlie and Ashley 2019; Knist et al. 2020). Decreasing rates of convective initiation and resulting precipitation may have long-term implications for agriculture and water availability. While a degree of caution must be stressed when using reanalysis data, our result reinforces the hypothesis that lower fraction of convective environments yield fewer thunderstorms in the present climate due to the significant increases in convective inhibition, and reductions in relative humidity.

These findings suggest that changes to severe thunderstorms are not straightforward, and increases inferred purely on the basis of unstable environments may be offset by the resistance to convection initiating. Therefore, a stronger emphasis should be placed on the convective initiation problem in future analyses of trends and projections, similar to the approach of Trapp and Hoogewind (2016) and Hoogewind et al. (2017). Since CIN depends on details in the thermodynamic structure in the lowest part of the atmosphere, its accurate calculation requires high resolution near the ground. In this context it is advisable to use native model levels for CIN computations, instead of basing it on less well-resolved pressure level data, which has been a typical practice in the past. Finally, the results here also highlight that regional factors play a significant role in convective trends, meaning that trends obtained over one region cannot necessarily be extrapolated to different parts of the world.

Acknowledgments. This research was supported by the grants from the Polish National Science Centre (Project 2017/27/B/ST10/00297) and the Polish National Agency for Academic Exchange—The Bekker Programme (Project PPN/BEK/2018/1/00199). The reanalysis and sounding computations were performed in the Poznań Supercomputing and Networking Center (Project 331). J. T. Allen acknowledges support from the National Science Foundation under Grant AGS-1945286.

Appendix A: MIXR for seasons

Figure A1 shows climatology and long-term trends in MIXR as in Fig. 1c, but for seasons.

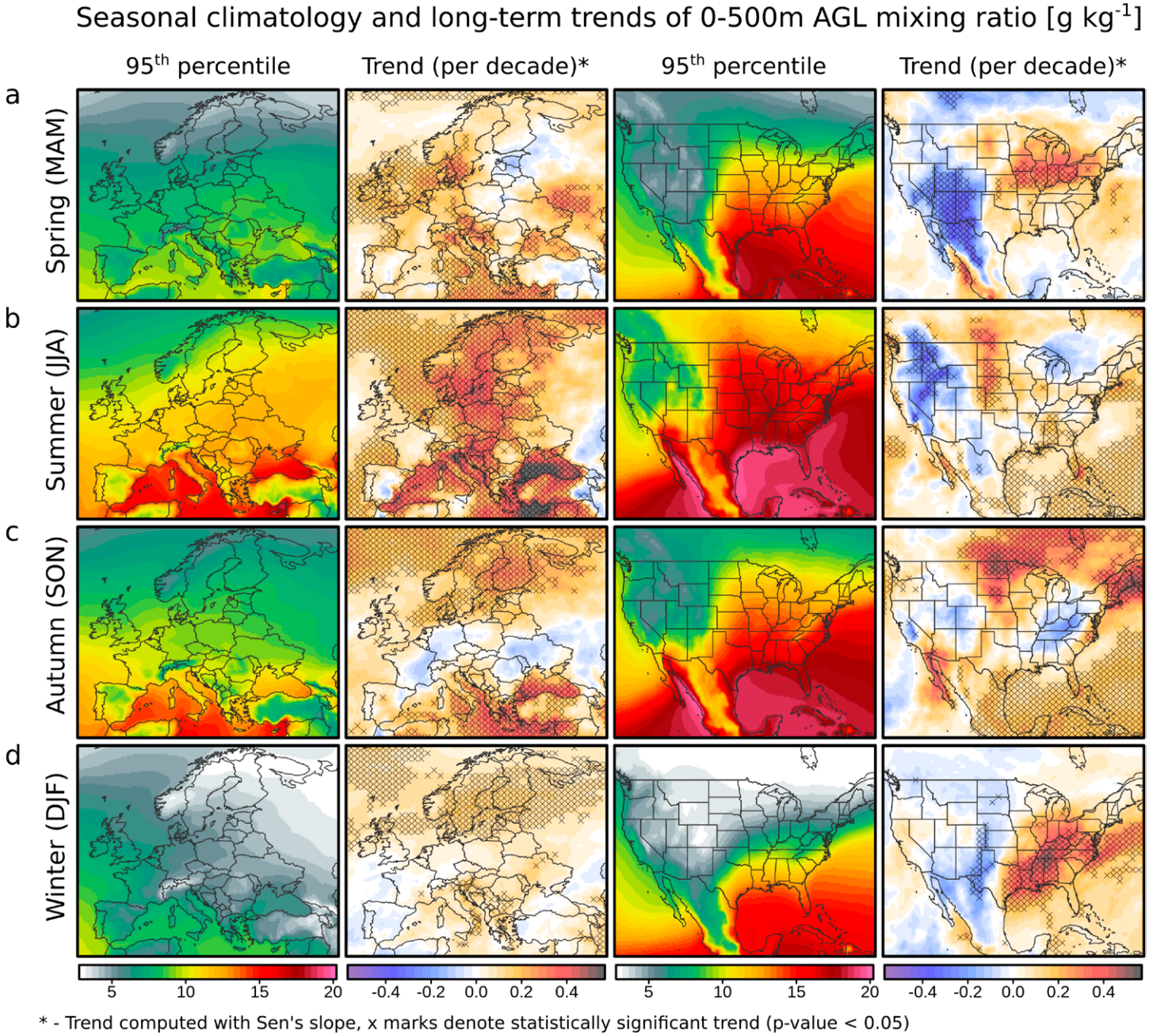

Fig. A1. As in Fig. 1c, but for seasons.

Appendix B: CAPE for seasons

Figure B1 shows climatology and long-term trends in CAPE as in Fig. 2a, but for seasons.

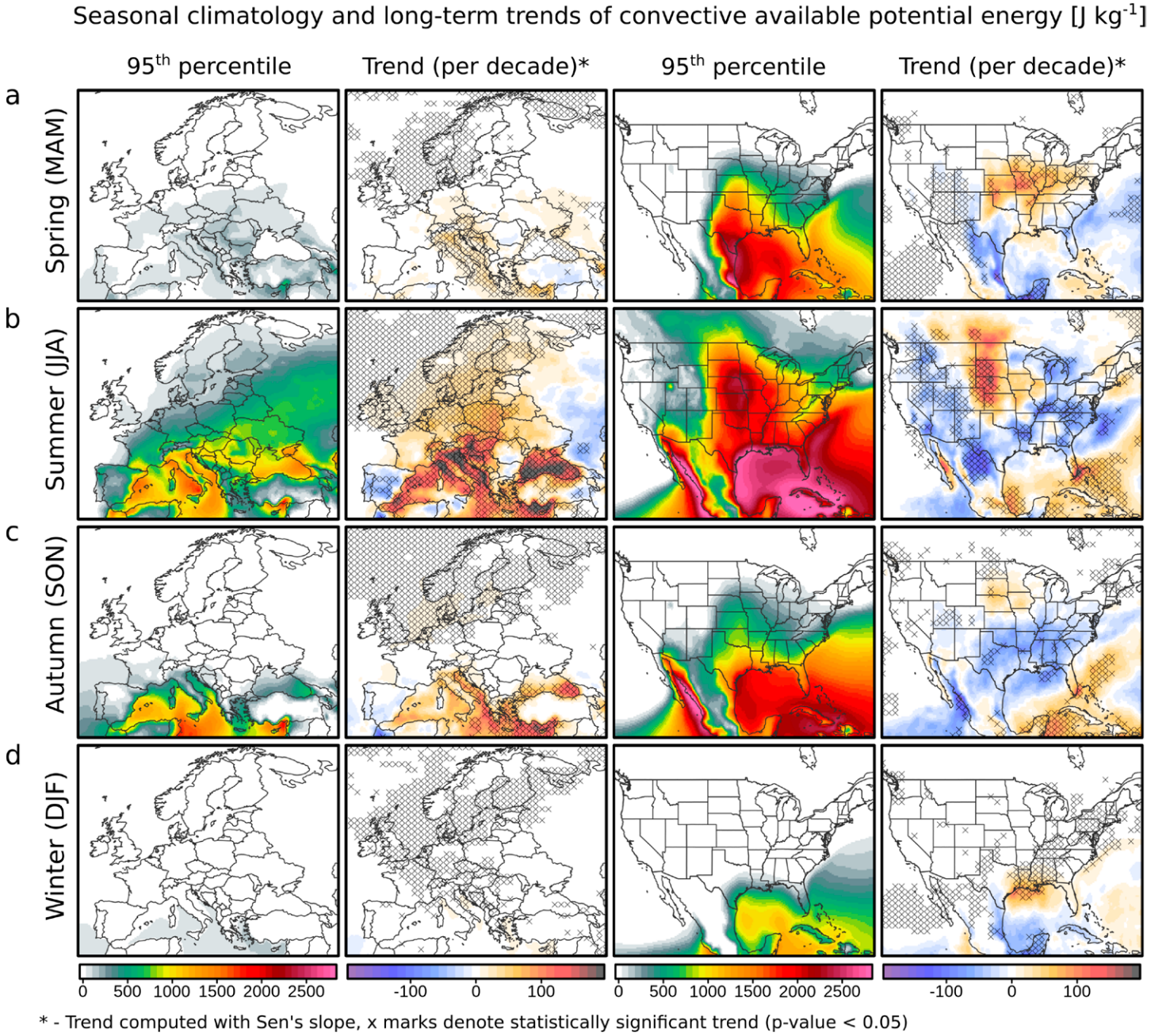

Fig. B1. As in Fig. 2a, but for seasons.

Appendix C: CIN for seasons

Figure C1 shows climatology and long-term trends in CIN as in Fig. 2b, but for seasons.

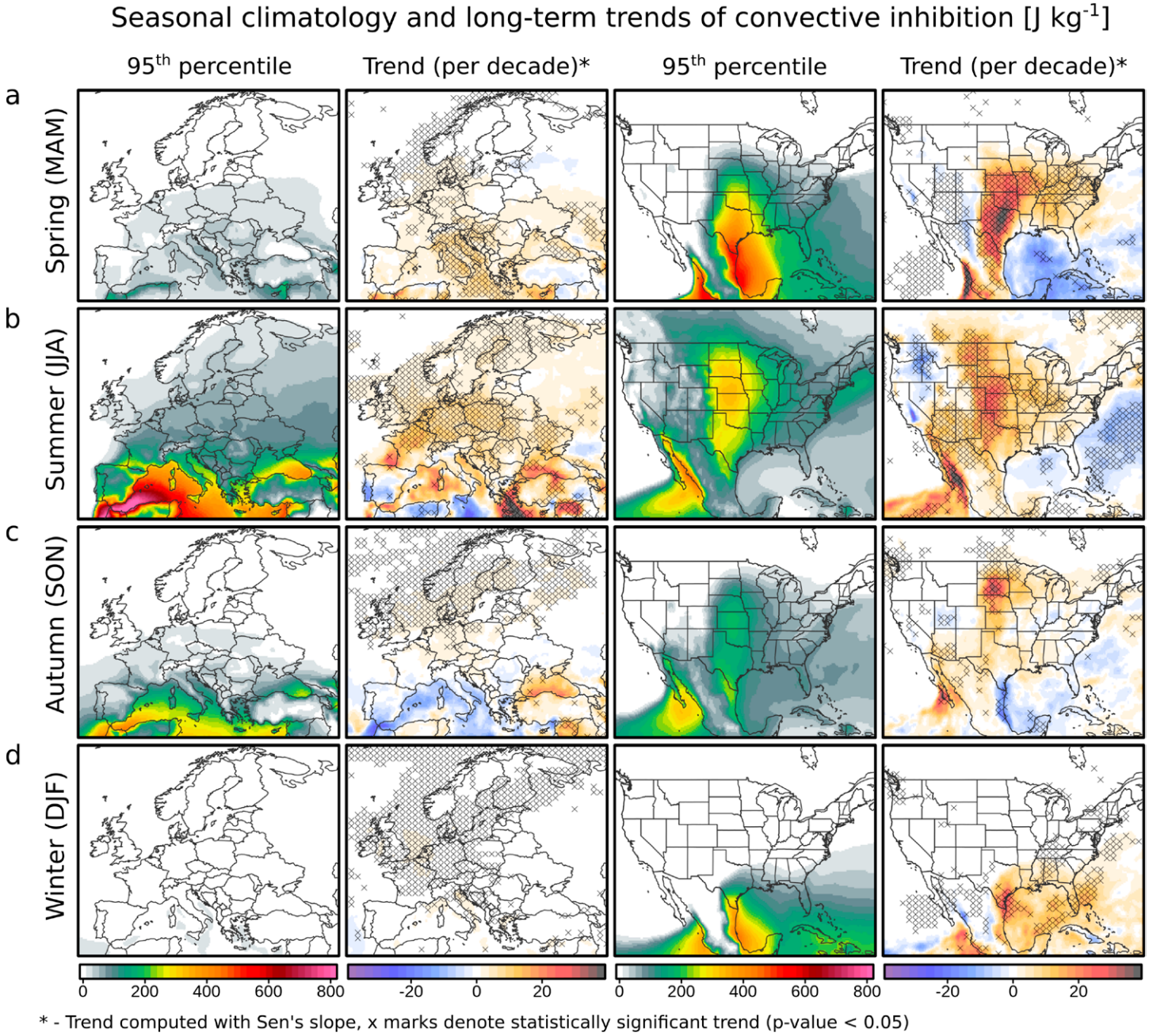

Fig. C1. As in Fig. 2b, but for seasons.

Appendix D: BS06 for seasons

Figure D1 shows climatology and long-term trends in BS06 as in Fig. 2c, but for seasons.

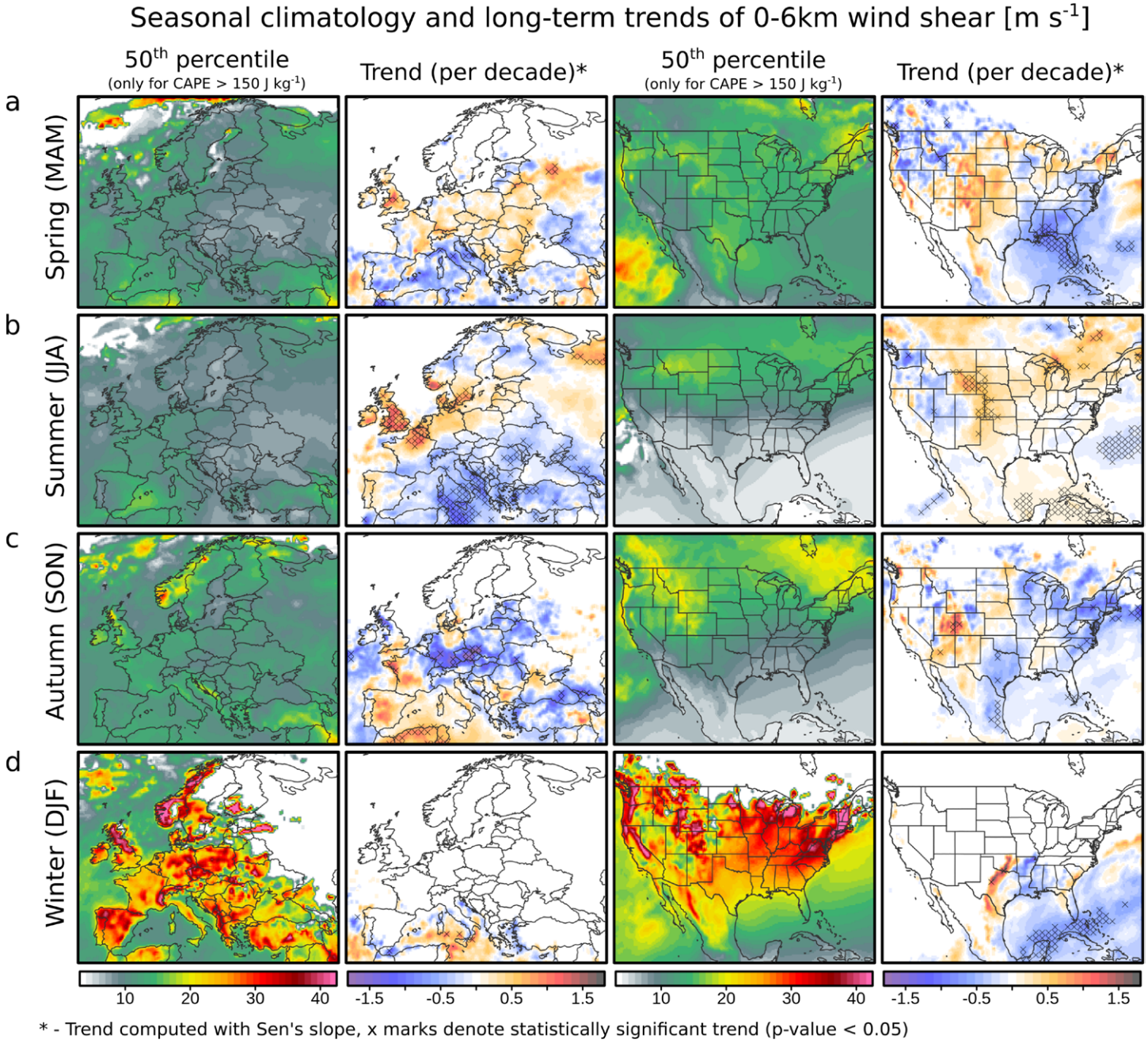

Fig. D1. As in Fig. 2c, but for seasons.

Appendix E: SRH03 for seasons

Figure E1 shows climatology and long-term trends in SRH03 as in Fig. 2d, but for seasons.

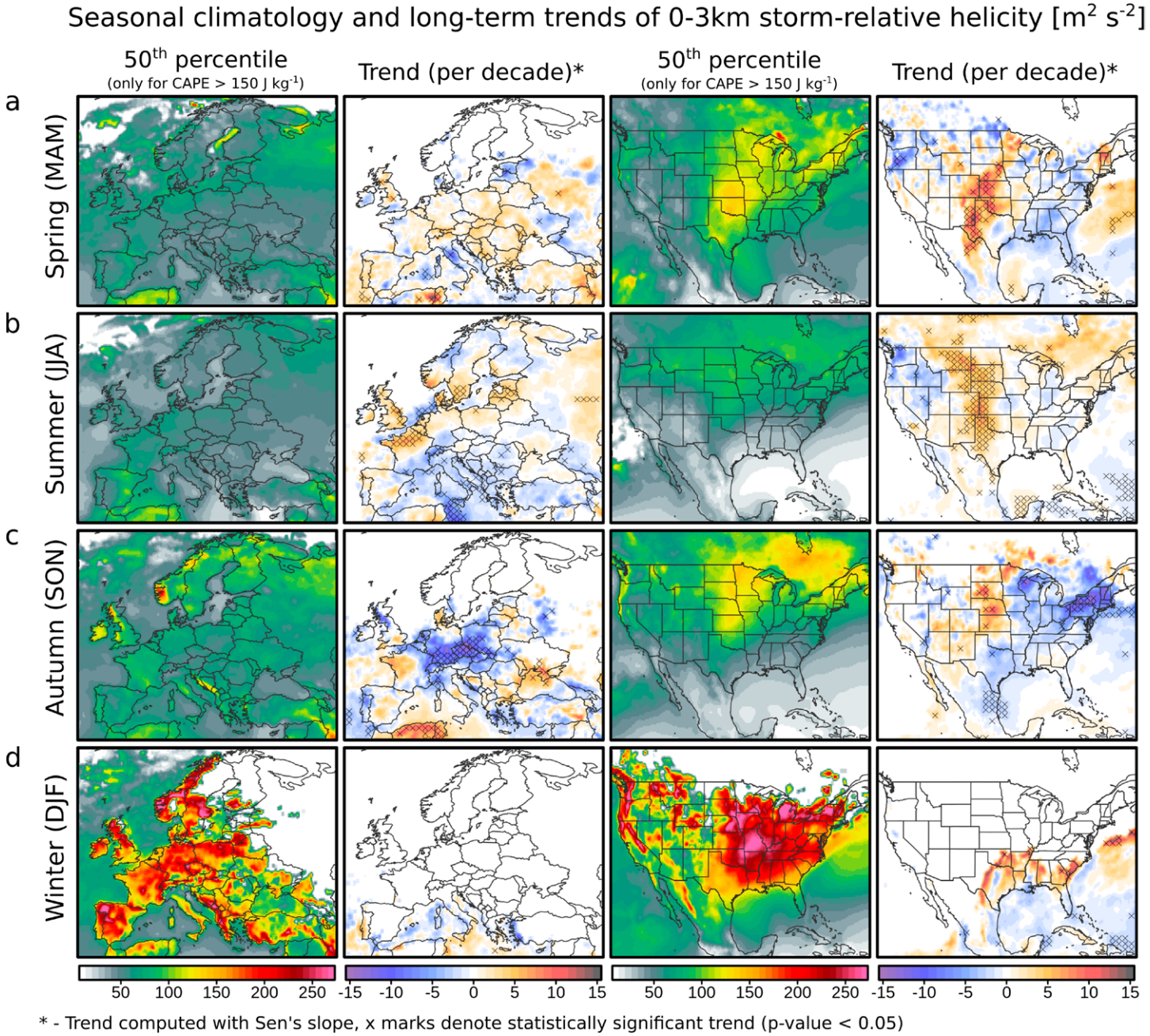

Fig. E1. As in Fig. 2d, but for seasons.

Appendix F: STP for seasons

Figure F1 shows climatology and long-term trends in STP as in Fig. 4c, but for seasons.

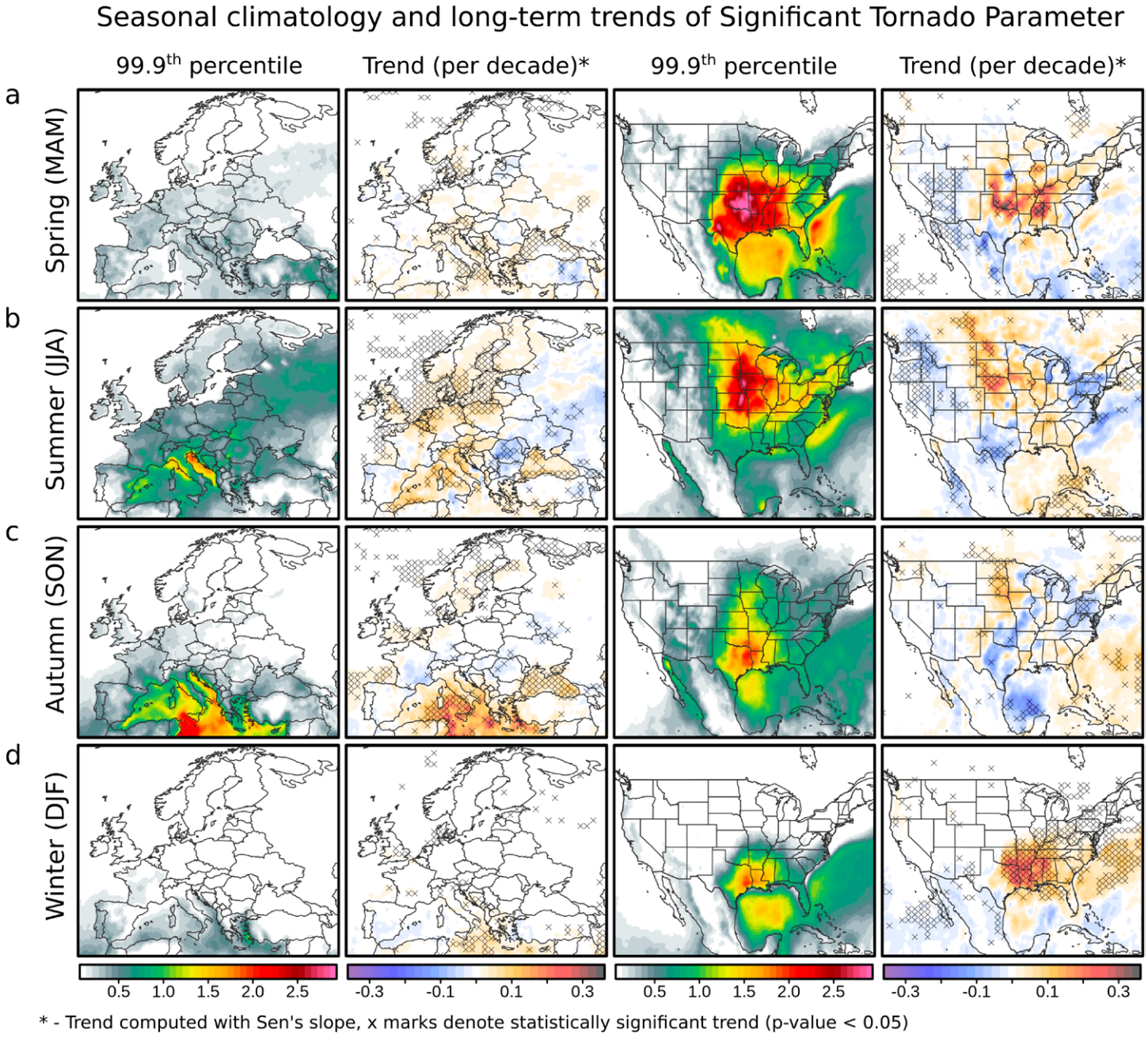

Fig. F1. As in Fig. 4c, but for seasons.

References

Agard, V., and K. Emanuel, 2017: Clausius–Clapeyron scaling of peak CAPE in continental convective storm environments. *J. Atmos. Sci.*, **74**, 3043–3054, https://doi.org/10.1175/JAS-D-16-0352.1.

Allen, J. T., 2018: Climate change and severe thunderstorms. *Oxford Research Encyclopedia of Climate Science*, Oxford University Press, https://doi.org/10.1093/acrefore/9780190228620.013.62.

——, and D. J. Karoly, 2014: A climatology of Australian severe thunderstorm environments 1979–2011: Inter-annual variability and ENSO influence. *Int. J. Climatol.*, **34**, 81–97, https://doi.org/10.1002/joc.3667.

——, and M. K. Tippett, 2015: The characteristics of United States hail reports: 1955-2014. *Electron. J. Severe Storms Meteor.*, **10** (3), www.ejssm.org/ojs/index.php/ejssm/article/viewArticle/149.

——, D. J. Karoly, and G. A. Mills, 2011: A severe thunderstorm climatology for Australia and associated thunderstorm environments. *Aust. Meteor. Oceanogr. J.*, **61**, 143–158, https://doi.org/10.22499/2.6103.001.

——, M. K. Tippett, and A. H. Sobel, 2015: Influence of the El Niño/Southern Oscillation on tornado and hail frequency in the United States. *Nat. Geosci.*, **8**, 278–283, https://doi.org/10.1038/ngeo2385.

——, I. M. Giammanco, M. R. Kumjian, H. J. Punge, Q. Zhang, P. Groenemeijer, M. Kunz, and K. Ortega, 2020: Understanding hail in the Earth system. *Rev. Geophys.*, **58**, e2019RG000665, https://doi.org/10.1029/2019RG000665.

Antonescu, B., T. Púčik, and D. M. Schultz, 2020: Hindcasting the first tornado forecast in Europe: 25 June 1967. *Wea. Forecasting*, **35**, 417–436, https://doi.org/10.1175/WAF-D-19-0173.1.

Archer, C. L., and K. Caldeira, 2008: Historical trends in the jet streams. *Geophys. Res. Lett.*, **35**, L08803, https://doi.org/10.1029/2008GL033614.

Banacos, P. C., and M. L. Ekster, 2010: The association of the elevated mixed layer with significant severe weather events in the northeastern United States. *Wea. Forecasting*, **25**, 1082–1102, https://doi.org/10.1175/2010WAF2222363.1.

Barandiaran, D., S. Y. Wang, and K. Hilburn, 2013: Observed trends in the Great Plains low-level jet and associated precipitation changes in relation to recent droughts. *Geophys. Res. Lett.*, **40**, 6247–6251, https://doi.org/10.1002/2013GL058296.

Bechtold, P., N. Semane, P. Lopez, J. Chaboureau, A. Beljaars, and N. Bormann, 2014: Representing equilibrium and nonequilibrium convection in large-scale models. *J. Atmos. Sci.*, **71**, 734–753, https://doi.org/10.1175/JAS-D-13-0163.1.

Brooks, H. E., 2009: Proximity soundings for severe convection for Europe and the United States from reanalysis data. *Atmos. Res.*, **93**, 546–553, https://doi.org/10.1016/j.atmosres.2008.10.005.

——, 2013: Severe thunderstorms and climate change. *Atmos. Res.*, **123**, 129–138, https://doi.org/10.1016/j.atmosres.2012.04.002.

——, J. W. Lee, and J. P. Craven, 2003: The spatial distribution of severe thunderstorm and tornado environments from global reanalysis data. *Atmos. Res.*, **67–68**, 73–94, https://doi.org/10.1016/S0169-8095(03)00045-0.

——, G. W. Carbin, and P. T. Marsh, 2014: Increased variability of tornado occurrence in the United States. *Science*, **346**, 349–352, https://doi.org/10.1126/science.1257460.

Bunkers, M. J., B. A. Klimowski, J. W. Zeitler, R. L. Thompson, and M. L. Weisman, 2000: Predicting supercell motion using a new hodograph technique. *Wea. Forecasting*, **15**, 61–79, https://doi.org/10.1175/1520-0434(2000)015<0061:PSMUAN>2.0.CO;2.

——, J. R. Wetenkamp, J. J. Schild, and A. Fischer, 2010: Observations of the relationship between 700-mb temperatures and severe weather reports across the contiguous United States. *Wea. Forecasting*, **25**, 799–814, https://doi.org/10.1175/2009WAF2222333.1.

Byrne, M. P., and P. A. O'Gorman, 2016: Understanding decreases in land relative humidity with global warming: Conceptual model and GCM simulations. *J. Climate*, **29**, 9045–9061, https://doi.org/10.1175/JCLI-D-16-0351.1.

Carlson, T. N., and F. H. Ludlam, 1968: Conditions for the occurrence of severe local storms. *Tellus*, **20**, 203–226, https://doi.org/10.3402/tellusa.v20i2.10002.

Chen, J., A. Dai, Y. Zhang, and K. L. Rasmussen, 2020: Changes in convective available potential energy and convective inhibition under global warming. *J. Climate*, **33**, 2025–2050, https://doi.org/10.1175/JCLI-D-19-0461.1.

Chernokulsky, A., F. Kozlov, O. Zolina, O. N. Bulygina, I. Mokhov, and V. Semenov, 2019: Observed changes in convective and stratiform precipitation in northern Eurasia over the last five decades. *Environ. Res. Lett.*, **14**, 045001, https://doi.org/10.1088/1748-9326/aafb82.

——, and Coauthors, 2020: Tornadoes in northern Eurasia: From the Middle Age to the Information Era. *Mon. Wea. Rev.*, **148**, 3081–3110, https://doi.org/10.1175/MWR-D-19-0251.1.

Coffer, B. E., M. D. Parker, R. L. Thompson, B. T. Smith, and R. E. Jewell, 2019: Using near-ground storm relative helicity in supercell tornado forecasting. *Wea. Forecasting*, **34**, 1417–1435, https://doi.org/10.1175/WAF-D-19-0115.1.

Cook, K. H., E. K. Vizy, Z. S. Launer, and C. M. Patricola, 2008: Springtime intensification of the Great Plains low-level jet and Midwest precipitation in GCM simulations of the twenty-first century. *J. Climate*, **21**, 6321–6340, https://doi.org/10.1175/2008JCLI2355.1.

Coumou, D., J. Lehmann, and J. Beckmann, 2015: The weakening summer circulation in the Northern Hemisphere mid-latitudes. *Science*, **348**, 324–327, https://doi.org/10.1126/science.1261768.

Craven, J. P., and H. E. Brooks, 2004: Baseline climatology of sounding derived parameters associated with deep, moist convection. *Natl. Wea. Dig.*, **28**, 13–24, http://nwafiles.nwas.org/digest/papers/2004/Vol28/Pg13-Craven.pdf.

Cummins, K. L., and M. J. Murphy, 2009: An overview of lightning locating systems: History, techniques, and data uses, with an in-depth look at the US NLDN. *IEEE Trans. Electromagn. Compat.*, **51**, 499–518, https://doi.org/10.1109/TEMC.2009.2023450.

Del Genio, A. D., M.-S. Yao, and J. Jonas, 2007: Will moist convection be stronger in a warmer climate? *Geophys. Res. Lett.*, **34**, L16703, https://doi.org/10.1029/2007GL030525.

Diffenbaugh, N. S., M. Scherer, and R. J. Trapp, 2013: Robust increases in severe thunderstorm environments in response to greenhouse forcing. *Proc. Natl. Acad. Sci. USA*, **110**, 16361–16366, https://doi.org/10.1073/pnas.1307758110.

Doswell, C. A., III, and E. N. Rasmussen, 1994: The effect of neglecting the virtual temperature correction on CAPE calculations. *Wea. Forecasting*, **9**, 625–629, https://doi.org/10.1175/1520-0434(1994)009<0625:TEONTV>2.0.CO;2.

——, H. E. Brooks, and R. A. Maddox, 1996: Flash flood forecasting: An ingredients-based methodology. *Wea. Forecasting*, **11**, 560–581, https://doi.org/10.1175/1520-0434(1996)011<0560:FFFAIB>2.0.CO;2.

Edwards, R., J. T. Allen, and G. W. Carbin, 2018: Reliability and climatological impacts of convective wind estimations. *J. Appl. Meteor. Climatol.*, **57**, 1825–1845, https://doi.org/10.1175/JAMC-D-17-0306.1.

Elsner, J. B., S. C. Elsner, and T. H. Jagger, 2015: The increasing efficiency of tornado days in the United States. *Climate Dyn.*, **45**, 651–659, https://doi.org/10.1007/s00382-014-2277-3.

Emanuel, K. A., 1994: *Atmospheric Convection*. Oxford University Press, 592 pp.

Gatzen, C. P., A. H. Fink, D. M. Schultz, and J. G. Pinto, 2020: An 18-year climatology of derechos in Germany. *Nat. Hazards Earth Syst. Sci.*, **20**, 1335–1351, https://doi.org/10.5194/nhess-20-1335-2020.

Gensini, V. A., and W. S. Ashley, 2011: Climatology of potentially severe convective environments from the North American Regional Reanalysis. *Electron. J. Severe Storms Meteor.*, **6** (8), www.ejssm.org/ojs/index.php/ejssm/article/viewArticle/85.

——, and T. L. Mote, 2015: Downscaled estimates of late 21st century severe weather from CCSM3. *Climatic Change*, **129**, 307–321, https://doi.org/10.1007/s10584-014-1320-z.

——, and H. E. Brooks, 2018: Spatial trends in United States tornado frequency. *npj Climate Atmos. Sci.*, **1**, 38, https://doi.org/10.1038/s41612-018-0048-2.

——, and L. Bravo de Guenni, 2019: Environmental covariate representation of seasonal U.S. tornado frequency. *J. Appl. Meteor. Climatol.*, **58**, 1353–1367, https://doi.org/10.1175/JAMC-D-18-0305.1.

——, T. L. Mote, and H. E. Brooks, 2014: Severe-thunderstorm reanalysis environments and collocated radiosonde observations. *J. Appl. Meteor. Climatol.*, **53**, 742–751, https://doi.org/10.1175/JAMC-D-13-0263.1.

Grams, J. S., R. L. Thompson, D. V. Snively, J. A. Prentice, G. M. Hodges, and L. J. Reames, 2012: A climatology and comparison of parameters for significant tornado events in the United States. *Wea. Forecasting*, **27**, 106–123, https://doi.org/10.1175/WAF-D-11-00008.1.

Groenemeijer, P., and Coauthors, 2017: Severe convective storms in Europe: Ten years of research and education at the European Severe Storms Laboratory. *Bull. Amer. Meteor. Soc.*, **98**, 2641–2651, https://doi.org/10.1175/BAMS-D-16-0067.1.

Gropp, M. E., and C. E. Davenport, 2018: The impact of the nocturnal transition on the lifetime and evolution of supercell thunderstorms in the Great Plains. *Wea. Forecasting*, **33**, 1045–1061, https://doi.org/10.1175/WAF-D-17-0150.1.

Guastini, C. T., and L. F. Bosart, 2016: Analysis of a progressive derecho climatology and associated formation environments. *Mon. Wea. Rev.*, **144**, 1363–1382, https://doi.org/10.1175/MWR-D-15-0256.1.

Haberlie, A. M., and W. S. Ashley, 2019: A radar-based climatology of mesoscale convective systems in the United States. *J. Climate*, **32**, 1591–1606, https://doi.org/10.1175/JCLI-D-18-0559.1.

Hersbach, H., and Coauthors, 2020: The ERA5 global reanalysis. *Quart. J. Roy. Meteor. Soc.*, **146**, 1999–2049, https://doi.org/10.1002/QJ.3803.

Hoogewind, K. A., M. E. Baldwin, and R. J. Trapp, 2017: The impact of climate change on hazardous convective weather in the United States: Insight from high-resolution dynamical downscaling. *J. Climate*, **30**, 10081–10100, https://doi.org/10.1175/JCLI-D-16-0885.1.

IPCC, 2018: *Global Warming of 1.5°C*. IPCC, 630 pp.

Johns, R. H., and C. A. I. I. I. Doswell, 1992: Severe local storms forecasting. *Wea. Forecasting*, **7**, 588–612, https://doi.org/10.1175/1520-0434(1992)007<0588:SLSF>2.0.CO;2.

Kaltenböck, R., G. Diendorfer, and N. Dotzek, 2009: Evaluation of thunderstorm indices from ECMWF analyses, lightning data and severe storm reports. *Atmos. Res.*, **93**, 381–396, https://doi.org/10.1016/j.atmosres.2008.11.005.

King, A. T., and A. D. Kennedy, 2019: North American supercell environments in atmospheric reanalyses and RUC-2. *J. Appl. Meteor. Climatol.*, **58**, 71–92, https://doi.org/10.1175/JAMC-D-18-0015.1.

Kingfield, D. M., K. M. Calhoun, and K. M. de Beurs, 2017: Antenna structures and cloud-to-ground lightning location: 1995–2015. *Geophys. Res. Lett.*, **44**, 5203–5212, https://doi.org/10.1002/2017GL073449.

Knist, S., K. Goergen, and C. Simmer, 2020: Evaluation and projected changes of precipitation statistics in convection-permitting WRF climate simulations over central Europe. *Climate Dyn.*, **55**, 325–341, https://doi.org/10.1007/s00382-018-4147-x.

Koehler, T. L., 2020: Cloud-to-ground lightning flash density and thunderstorm day distributions over the contiguous United States derived from NLDN measurements: 1993–2018. *Mon. Wea. Rev.*, **148**, 313–332, https://doi.org/10.1175/MWR-D-19-0211.1.

Kolendowicz, L., 2012: Synoptic patterns associated with thunderstorms in Poland. *Meteor. Z.*, **21**, 145–156, https://doi.org/10.1127/0941-2948/2012/0272.

Mahoney, K., 2020: Extreme hail storms and climate change: Foretelling the future in tiny, turbulent crystal balls? *Bull. Amer. Meteor. Soc.*, **101**, S17–S22, https://doi.org/10.1175/BAMS-D-19-0233.1.

Medici, G., K. L. Cummins, D. J. Cecil, W. J. Koshak, and S. D. Rudlosky, 2017: The intracloud lightning fraction in the contiguous United States. *Mon. Wea. Rev.*, **145**, 4481–4499, https://doi.org/10.1175/MWR-D-16-0426.1.

Mohr, S., and M. Kunz, 2013: Recent trends and variabilities of convective parameters relevant for hail events in Germany and Europe. *Atmos. Res.*, **123**, 211–228, https://doi.org/10.1016/j.atmosres.2012.05.016.

——, ——, and K. Keuler, 2015: Development and application of a logistic model to estimate the past and future hail potential in Germany. *J. Geophys. Res. Atmos.*, **120**, 3939–3956, https://doi.org/10.1002/2014JD022959.

Molina, M. J., and J. T. Allen, 2020: Regionally-stratified tornadoes: Moisture source physical reasoning and climate trends. *Wea. Climate Extremes*, **28**, 100244, https://doi.org/10.1016/j.wace.2020.100244.

Murphy, M., and A. Nag, 2015: Cloud lightning performance and climatology of the U.S. based on the upgraded U.S. National Lightning Detection Network. *Seventh Conf. on the Meteorological Applications of Lightning Data*, Phoenix, AZ, Amer. Meteor. Soc., 8.2, https://ams.confex.com/ams/95Annual/webprogram/Paper262391.html.

Orville, R. E., 1991: Lightning ground flash density in the contiguous United States—1989. *Mon. Wea. Rev.*, **119**, 573–577, https://doi.org/10.1175/1520-0493(1991)119<0573:LGFDIT>2.0.CO;2.

Parding, K. M., R. Benestad, A. Mezghani, and H. B. Erlandsen, 2019: Statistical projection of the North Atlantic storm tracks. *J. Appl. Meteor. Climatol.*, **58**, 1509–1522, https://doi.org/10.1175/JAMC-D-17-0348.1.

Pena-Ortiz, C., D. Gallego, P. Ribera, P. Ordonez, and M. D. C. Alvarez-Castro, 2013: Observed trends in the global jet stream characteristics during the second half of the 20th century. *J. Geophys. Res. Atmos.*, **118**, 2702–2713, https://doi.org/10.1002/JGRD.50305.

Piper, D., M. Kunz, J. T. Allen, and S. Mohr, 2019: Investigation of the temporal variability of thunderstorms in central and western Europe and the relation to large scale flow and teleconnection patterns. *Quart. J. Roy. Meteor. Soc.*, **145**, 3644–3666, https://doi.org/10.1002/qj.3647.

Pistotnik, G., P. Groenemeijer, and R. Sausen, 2016: Validation of convective parameters in MPI-ESM decadal hindcasts (1971–2012) against ERA-Interim reanalyses. *Meteor. Z.*, **25**, 753–766, https://doi.org/10.1127/metz/2016/0649.

Púčik, T., P. Groenemeijer, D. Rýva, and M. Kolář, 2015: Proximity soundings of severe and nonsevere thunderstorms in central Europe. *Mon. Wea. Rev.*, **143**, 4805–4821, https://doi.org/10.1175/MWR-D-15-0104.1.

——, and Coauthors, 2017: Future changes in European severe convection environments in a regional climate model ensemble. *J. Climate*, **30**, 6771–6794, https://doi.org/10.1175/JCLI-D-16-0777.1.

Punkka, A., and M. Bister, 2005: Occurrence of summertime convective precipitation and mesoscale convective systems in Finland during 2000–01. *Mon. Wea. Rev.*, **133**, 362–373, https://doi.org/10.1175/MWR-2854.1.

Rädler, A. T., P. Groenemeijer, E. Faust, and R. Sausen, 2018: Detecting severe weather trends using an additive regressive convective hazard model (ARCHaMo). *J. Appl. Meteor. Climatol.*, **57**, 569–587, https://doi.org/10.1175/JAMC-D-17-0132.1.

——, ——, ——, ——, and T. Púčik, 2019: Frequency of severe thunderstorms across Europe expected to increase in the 21st century due to rising instability. *npj Climate Atmos. Sci.*, **2**, 30, https://doi.org/10.1038/s41612-019-0083-7.

Rasmussen, K. L., A. F. Prein, R. M. Rasmussen, K. Ikeda, and C. Liu, 2020: Changes in the convective population and thermodynamic environments in convection-permitting regional climate simulations over the United States. *Climate Dyn.*, **55**, 383–408, https://doi.org/10.1007/s00382-017-4000-7.

Robinson, E. D., R. J. Trapp, and M. E. Baldwin, 2013: The geospatial and temporal distributions of severe thunderstorms from high-resolution dynamical downscaling. *J. Appl. Meteor. Climatol.*, **52**, 2147–2161, https://doi.org/10.1175/JAMC-D-12-0131.1.

Rodriguez, O., and J. Bech, 2018: Sounding-derived parameters associated with tornadic storms in Catalonia. *Int. J. Climatol.*, **38**, 2400–2414, https://doi.org/10.1002/joc.5343.

Romps, D. M., J. T. Seeley, D. Vollaro, and J. Molinari, 2014: Projected increase in lightning strikes in the United States due to global warming. *Science*, **346**, 851–854, https://doi.org/10.1126/science.1259100.

Sepp, M., P. Post, and J. Jaagus, 2005: Long-term changes in the frequency of cyclones and their trajectories in central and northern Europe. *Hydrol. Res.*, **36**, 297–309, https://doi.org/10.2166/nh.2005.0023.

Smith, B. T., R. L. Thompson, J. S. Grams, C. Broyles, and H. E. Brooks, 2012: Convective modes for significant severe thunderstorms in the contiguous United States. Part I: Storm classification and climatology. *Wea. Forecasting*, **27**, 1114–1135, https://doi.org/10.1175/WAF-D-11-00115.1.

Tang, B. H., V. A. Gensini, and C. R. Homeyer, 2019: Trends in United States large hail environments and observations. *npj Climate Atmos. Sci.*, **2**, 45, https://doi.org/10.1038/s41612-019-0103-7.

Tang, Y., J. Winkler, S. Zhong, X. Bian, D. Doubler, L. Yu, and C. Walters, 2017: Future changes in the climatology of the Great Plains low-level jet derived from fine resolution multi-model simulations. *Sci. Rep.*, **7**, 5029, https://doi.org/10.1038/S41598-017-05135-0.

Taszarek, M., H. E. Brooks, and B. Czernecki, 2017: Sounding-derived parameters associated with convective hazards in Europe. *Mon. Wea. Rev.*, **145**, 1511–1528, https://doi.org/10.1175/MWR-D-16-0384.1.

——, ——, ——, P. Szuster, and K. Fortuniak, 2018: Climatological aspects of convective parameters over Europe: A comparison of ERA-Interim and sounding data. *J. Climate*, **31**, 4281–4308, https://doi.org/10.1175/JCLI-D-17-0596.1.

——, and Coauthors, 2019: A climatology of thunderstorms across Europe from a synthesis of multiple data sources. *J. Climate*, **32**, 1813–1837, https://doi.org/10.1175/JCLI-D-18-0372.1.

——, S. Kendzierski, and N. Pilguj, 2020: Hazardous weather affecting European airports: Climatological estimates of situations with limited visibility, thunderstorm, low-level wind shear and snowfall from ERA5. *Wea. Climate Extremes*, **28**, 100243, https://doi.org/10.1016/j.wace.2020.100243.

Thompson, R. L., B. T. Smith, J. S. Grams, A. R. Dean, and C. Broyles, 2012: Convective modes for significant severe thunderstorms in the contiguous United States. Part II: Supercell and QLCS tornado environments. *Wea. Forecasting*, **27**, 1136–1154, https://doi.org/10.1175/WAF-D-11-00116.1.

Tippett, M. K., and W. J. Koshak, 2018: A baseline for the predictability of U.S. cloud-to-ground lightning. *Geophys. Res. Lett.*, **45**, 10 719–10 728, https://doi.org/10.1029/2018GL079750.

——, A. H. Sobel, and S. J. Camargo, 2012: Association of U.S. tornado occurrence with monthly environmental parameters. *Geophys. Res. Lett.*, **39**, L02801, https://doi.org/10.1029/2011GL050368.

——, C. Lepore, and J. E. Cohen, 2016: More tornadoes in the most extreme US tornado outbreaks. *Science*, **354**, 1419–1423, https://doi.org/10.1126/science.aah7393.

——, ——, W. J. Koshak, T. Chronis, and B. Vant-Hull, 2019: Performance of a simple reanalysis proxy for US cloud-to-ground lightning. *Int. J. Climatol.*, **39**, 3932–3946, https://doi.org/10.1002/joc.6049.

Trapp, R. J., and K. A. Hoogewind, 2016: The realization of extreme tornadic storm events under future anthropogenic climate change. *J. Climate*, **29**, 5251–5265, https://doi.org/10.1175/JCLI-D-15-0623.1.

——, N. S. Diffenbaugh, H. E. Brooks, M. E. Baldwin, E. D. Robinson, and J. S. Pal, 2007: Changes in severe thunderstorm environment frequency during the 21st century caused by anthropogenically enhanced global radiative forcing. *Proc. Natl. Acad. Sci. USA*, **104**, 19 719–19 723, https://doi.org/10.1073/pnas.0705494104.

——, ——, and A. Gluhovsky, 2009: Transient response of severe thunderstorm forcing to elevated greenhouse gas concentrations. *Geophys. Res. Lett.*, **36**, L01703, https://doi.org/10.1029/2008GL036203.

——, K. A. Hoogewind, and S. Lasher-Trapp, 2019: Future changes in hail occurrence in the United States determined through convection-permitting dynamical downscaling. *J. Climate*, **32**, 5493–5509, https://doi.org/10.1175/JCLI-D-18-0740.1.

van Delden, A., 2001: The synoptic setting of thunderstorms in western Europe. *Atmos. Res.*, **56**, 89–110, https://doi.org/10.1016/S0169-8095(00)00092-2.

van den Broeke, M. S., D. M. Schultz, R. H. Johns, J. S. Evans, and J. E. Hales, 2005: Cloud-to-ground lightning production in strongly forced, low-instability convective lines associated with damaging wind. *Wea. Forecasting*, **20**, 517–530, https://doi.org/10.1175/WAF876.1.

Wacker, R. S., and R. E. Orville, 1999: Changes in measured lightning flash count and return stroke peak current after the 1994 U. S. National Lightning Detection Network upgrade. II. Theory. *J. Geophys. Res.*, **104**, 2159–2162, https://doi.org/10.1029/1998JD200059.

Wapler, K., and P. James, 2015: Thunderstorm occurrence and characteristics in central Europe under different synoptic conditions. *Atmos. Res.*, **158–159**, 231–244, https://doi.org/10.1016/j.atmosres.2014.07.011.

Weisman, M. L., and J. B. Klemp, 1982: The dependence of numerically simulated convective storms on vertical wind shear and buoyancy. *Mon. Wea. Rev.*, **110**, 504–520, https://doi.org/10.1175/1520-0493(1982)110<0504:TDONSC>2.0.CO;2.

Westermayer, A., P. Groenemeijer, G. Pistotnik, R. Sausen, and E. Faust, 2017: Identification of favorable environments for thunderstorms in reanalysis data. *Meteor. Z.*, **26**, 59–70, https://doi.org/10.1127/metz/2016/0754.

Wilcox, R. R., 2010: *Fundamentals of Modern Statistical Methods: Substantially Improving Power and Accuracy*. Springer, 249 pp.